Lilienkamp, Arne; Namocke, Nils

Working Paper

Integrating EVs into distribution grids: Examining the effects of various DSO intervention strategies on optimized charging

EWI Working Paper, No. 01/24

Provided in Cooperation with:
Institute of Energy Economics at the University of Cologne (EWI)

Suggested Citation: Lilienkamp, Arne; Namocke, Nils (2024) : Integrating EVs into distribution grids: Examining the effects of various DSO intervention strategies on optimized charging, EWI Working Paper, No. 01/24, Institute of Energy Economics at the University of Cologne (EWI), Cologne

This Version is available at:
https://hdl.handle.net/10419/286402

Integrating EVs into distribution grids – Examining the effects of various DSO intervention strategies on optimized charging

AUTHORS

Arne Lilienkamp

Nils Namockel

EWI Working Paper, No 01/24

January 2024

Institute of Energy Economics at the University of Cologne (EWI)
www.ewi.uni-koeln.de

Institute of Energy Economics
at the University of Cologne (EWI)

Alte Wagenfabrik
Vogelsanger Str. 321a
50827 Köln
Germany

Tel.: +49 (0)221 277 29-100
Fax: +49 (0)221 277 29-400
www.ewi.uni-koeln.de

CORRESPONDING AUTHOR

Arne Lilienkamp
Arne.lilienkamp@ewi.uni-koeln.de

ISSN: 1862-3808

Integrating EVs into distribution grids – Examining the effects of various DSO intervention strategies on optimized charging

Arne Lilienkamp[a,b,*], Nils Namockel[a,b]

[a] *Institute of Energy Economics at the University of Cologne, Vogelsanger Strasse 321a, 50827 Cologne, Germany.*
[b] *Chair of Energy Economics, University of Cologne, Vogelsanger Strasse 321a, 50827 Cologne, Germany.*

Abstract

Adopting electric vehicles (EVs) and implementing variable electricity tariffs increase peak demand and the risk of congestion in distribution grids. To avert critical grid situations and sidestep expensive grid expansions, Distribution System Operators (DSOs) must have intervention rights, allowing them to curtail charging processes. Various curtailment strategies are possible, varying in spatio-temporal differentiation and possible discrimination. However, evaluating different strategies is complex due to the interplay of economic factors, technical requirements, and regulatory constraints — a complexity not fully addressed in the current literature. Our study introduces a sophisticated model to optimize electric vehicle charging strategies to address this gap. This model considers different tariff schemes (Fixed, Time-of-Use, and Real-Time) and incorporates DSO interventions (basic, variable, and smart) within its optimization framework. Based on the model, we analyze the flexibility demand and total electricity costs from the users' perspective. Applying our model to a synthetic distribution grid, we find that flexible tariffs offer consumers only marginal economic benefits and increase the risk of grid congestion due to herding behavior. All curtailment strategies effectively alleviate congestion, with variable curtailment featuring spatio-temporal differentiation, approaching optimality regarding flexibility demand. Notably, applying curtailment from the users' perspective does not lower cost savings significantly.

Keywords: Distribution Grid, Electric Vehicles, Smart Charging, Flexibility

JEL classification: C61, D47, Q41, Q48

The contents of this paper reflect the opinions of its authors only and not those of EWI or University of Cologne.

*Corresponding author: *email*: arne.lilienkamp@ewi.uni-koeln.de. The authors are listed alphabetically by last name and contributed equally to this paper.

1. Introduction

As part of the global energy transition, there is a concerted effort to expand renewable energies (RES) and electrify various end-use sectors. Contributing to the ongoing electrification of the transportation sector, the increasing adoption of electric vehicles (EVs) plays a pivotal role in this transition. 14% of all new cars sold globally were electric in 2022, up from around 9% in 2021 and less than 5% in 2020. An even stronger increase is projected throughout 2023 (IEA, 2023b). Simultaneously, integrating digital technologies such as Smart Meters is a crucial component of the energy transition. Whereas some countries already experience a high penetration of smart meters, such as Italy, Sweden, Finland, or Spain, other countries plan to force the roll-out in the next years (Schnaars et al., 2022).

The digitization and the electrification of transportation not only underpin the shift towards cleaner energy sources but also results in sector coupling. Electric vehicles, with their increasing demand and through their interaction with the electricity system, will thus become an important actor within the future electricity system (IEA, 2023c). In this context, the ongoing digitization offers the prospect of employing electric vehicles in a way that actively supports and enhances the overall functionality of the electricity system. But, also, EV users can potentially benefit from exploiting the inherent flexibility of EVs (Englberger et al., 2021). By offering variable electricity tariffs to EV users, electricity providers can forward price signals from the electricity market, mirroring the state of the energy system. This has two implications. First, EV users can optimize their charging to minimize electricity costs, and second, the shifting of load implicitly contributes to balancing supply and demand in the energy system. For example, Schittekatte et al. (2022) show how time-of-use (TOU) tariffs incentivize load-shifting while simultaneously addressing consumer preferences.

Dynamic tariffs, however, abstract from the grid, as neither the retailers nor the consumers consider the grid infrastructure in their calculus. Given the divergent objectives of retailers, consumers, and grid operators, this poses a challenge and may lead to conflicts. Electric vehicle users prioritize low charging costs and meeting their mobility or electricity demand, while retailers align their tariffs with wholesale prices. In contrast, grid operators strive for stable grid operation. The pursuit of cost savings, often driven by a desire to benefit from low prices, can result in a high

simultaneity of charging processes among electric vehicle users, leading to load peaks that strain the grid infrastructure. This herding behavior poses a significant threat to distribution grids, where most electric vehicle demand is concentrated and becomes more pronounced with higher electric vehicle penetration rates. Grid congestion in distribution grids may occur, as highlighted by Valogianni et al. (2020) and Daneshzand et al. (2023).

To avoid grid congestion, three options exist in general. First, distribution system operators (DSOs) could restrict the access of EVs to the grid by limiting the installation of charging stations and wall boxes. This, however, is detrimental to the desired large-scale EV adoption and interferes with EV users' objectives. Second, DSOs could expand the grid so that even herding behavior does not cause congestion. However, designing a grid based on uncoordinated load peaks is considered a highly inefficient and overly expensive approach, especially as load peaks will increase in amplitude more than in frequency in the future (Arnold et al., 2023). Moreover, grid expansion faces delays in numerous countries and struggles to keep pace with the rising demand (IEA, 2023a). The third option involves granting DSOs the authority to intervene and limit EV charging during critical hours to prevent grid congestion, as proposed by (von Bonin et al., 2022). This can be achieved through methods such as volume signals. Actively restricting charging processes allows the grid operator to ensure stable grid operation, whereas passive solutions like time-varying grid fees may encourage herding behavior. While volume signals still impact EV users' goals, they represent a more cost-effective approach than extensive grid expansion, as demonstrated by (Spiliotis et al., 2016) and (Heilmann and Wozabal, 2021). The inconvenience of adjusting the charging strategy could be compensated, as proposed by Schittekatte et al. (2023). Consequently, the third option emerges as the most promising strategy for integrating more electric vehicles into distribution grids in the short and medium term, forming the central focus of this paper.

With an intervention, the actual charging strategy would need to be adjusted whenever bottlenecks in the distribution grid are imminent. The grid operator would thus have to influence the charging process by sending out signals. In electricity markets, where DSOs have to be unbundled, such as in Europe [1], grid operation and the optimization of EVs charging strategies have to take place

[1] Exceptions exist for DSOs with more than 100,000 customers European Comission (2010)

separately due to regulatory provisions. However, the current discussions revolve around granting the grid operator access to a certain extent, thereby considering constraints from grid operation in optimizing charging processes. Uncertainty surrounds how the grid operator gains influence over the charging process and how the characteristics of the grid can be taken into account in optimizing charging processes. In Germany, this discussion is taking place within the framework of the design of §14a EnWG (BNetzA, 2023). Here, the DSO could limit charging power with high grid utilization in certain hours. In summary, the different intervention options exhibit variability regarding the information involved, ranging from details about the grid utilization to individual load profiles and the potential for discrimination. All households could be treated equally, or the grid operator could possess the authority to exert individualized control.

Our paper contributes to the ongoing discussion by examining the effects of different intervention designs on optimal charging strategies within a case study centered on a synthetic German distribution grid. We aim to understand how various intervention options impact the optimal charging strategy. Initially, we identify optimal charging strategies based on different tariff designs, excluding considerations related to the grid. If grid congestion becomes a concern, we then introduce grid interventions through various curtailment strategies. We differentiate between generalized curtailment (treating all electric vehicle users equally behind the bottleneck) and differentiated curtailment (adjusting curtailment based on each user's impact on the bottleneck). Additionally, we explore exogenously fixed curtailment rates, independent of factors like current transformer overloads and endogenously variable curtailment rates, which depend on the real-time load. We address the following research questions: How do different tariff designs influence the optimal charging strategy of EV users and the resulting grid utilization? How do various DSO intervention rights affect the optimal charging strategy of EV users in terms of charging costs and required flexibility under different tariffs? Besides answering these questions, our research contributes to the existing literature as follows:

- Systematic analysis of mutual influences of charging strategies and interventions of grid operators

- Development of a model framework to analyze the interdependencies of users, retailers, and grid operators in distribution grids
- Application of the model framework to a case study for Germany based on a synthetic distribution grid
- Sensitivity analyses on the effect of different EV penetration rates

Consistent with prior research, such as von Bonin et al. (2022), our findings indicate that implementing time-variable tariffs brings financial advantages for consumers, but they are relatively minor. The weighted average cost savings reach 47.2 EUR per year in the case of Real-time tariffs and 16.9 EUR per year with ToU tariff, reflecting only 1 to 3% of total electricity costs. However, we find that time-variable tariffs, especially at high EV penetration rates, can lead to herding behavior and increase the peak load. To address this issue, DSOs need intervention rights to avoid grid congestion effectively. We show that all proposed intervention strategies are suitable to prevent congestion, although differences can be observed regarding their efficiency. The extent to which the DSO can convey differentiated signals, incorporating spatial and temporal differences, correlates closely with the optimal benchmark's accuracy, assuming perfect information and user discrimination. The choice of the curtailment strategy has a greater influence on the need for flexibility than the design of time-variable tariffs. From the end user's perspective, curtailment does not affect charging costs significantly, especially concerning ToU tariffs or low EV penetration rates. With RT tariffs and higher penetration rates, the choice of the curtailment strategy is more relevant. Then, basic curtailment increases charging costs by 4.7 EUR per year, while more sophisticated curtailment results in a slightly lower increase of 2.6 EUR per year. But still, from the end user's perspective, the financial benefits of smart tariffs outweigh the cost increase due to curtailment.

The paper is structured as follows. Chapter 2 introduces the electricity tariff designs and possibilities for DSO interventions. Chapter 3 details a method for modeling different grid intervention strategies in optimizing charging processes based on tariff designs. Chapter 4 applies this method to a synthetic distribution grid, while Chapter 5 discusses our findings. Chapter 6 concludes this paper.

2. Electricity tariff designs and possibilities for DSO interventions

The charging processes of electric vehicles can be controlled both passively and actively. With passive control, users are incentivized to shift their load, e.g., in response to price signals. Thus, users' charging decisions are influenced only indirectly. With active control, users' charging decisions can be overruled remotely, e.g., by volume signals to modulate the charging power of charging processes (IEA, 2022b). In this study, we analyze the interdependencies of time-varying electricity prices provided by retailers and volume signals from the DSO to curtail charging processes to avoid grid congestion. In this chapter, we introduce the different considered design options for these signals.

In terms of (retail) price signals, there are various tariff models with different structures, ranging from flat rates to piece-wise flat rates to fully dynamic pricing. The latter two belong to the group of (time-)variable price signals, which can help address the growing price volatility in wholesale markets while consumers can benefit economically. By shifting charging processes to periods of lower prices, charging processes are implicitly shifted according to the availability of intermittent resources (Schittekatte et al., 2022). In this paper, we distinguish three specific tariff designs: a Fixed tariff and two time-dependent tariffs known as Time-of-Use and Real-Time tariffs.

- **Fixed tariff**: Consumers pay the same electricity price regardless of when they consume electricity. Thus, Fixed tariffs do not incentivize a shift in charging processes. The retailer bears the price risk of the wholesale market but adds a risk premium to the tariff.

- **Time-of-Use tariff**: Time-of-Use tariffs provide time-variable electricity prices in certain predefined time windows. The tariffs segment the day into sections with equal price levels corresponding to the overall load (i.e., low, mid, and high). The differentiated prices incentivize a shift of charging processes into lower price windows.

- **Real-Time tariff**: Real-Time tariffs are fully time-variable, with the retailer forwarding volatile wholesale prices and price risk to the customers. However, if all EVs in a distribution grid receive the same high-resolution variable electricity price signal, it can lead to herding behavior and a high simultaneity of charging processes.

Responding to electricity price signals could result in herding behavior of charging processes, which may cause congestion issues in the distribution grid by concentrating charging power within specific time intervals. Consequently, the DSO may need to intervene actively and provide signals to electric vehicles, including curtailing their charging processes. To determine effective signals, the DSO requires access to information on grid utilization and user behavior, as well as the ability to interact with the charging stations of electric vehicles. In future energy systems, the level of digitization and the corresponding availability of information remains uncertain. Additionally, the treatment of charging stations, whether equal or individually controlled with possible discrimination, depends on the regulation of DSO. Consequently, various design options for DSO interventions are possible, differing regarding information availability and discrimination.

We consider three different curtailment strategies to reflect different intervention options: basic curtailment, variable curtailment, and smart curtailment.

- **Basic Curtailment**: Basic curtailment involves limiting charging processes based on anticipated congestion. DSOs use standard load profiles and probabilistic methods in non-digitized distribution grids to predict grid congestion. Once a DSO anticipates congestion in the distribution grid for a specified time interval, it can reduce the charging power of all charging stations downstream of the bottleneck. In this approach, the DSO applies the same fixed curtailment factor for the entire distribution grid. Charging processes are implicitly shifted to less critical time intervals by curtailing peak loads. However, this approach can be overly restrictive and may result in inefficiencies.

- **Variable Curtailment**: Variable curtailment builds upon the Basic Curtailment approach but introduces time-dependent curtailment signals. Instead of applying a fixed curtailment factor for the entire distribution grid, the DSO selectively curtails only the electric vehicles behind the anticipated bottleneck as necessary. Consequently, all users behind the bottleneck are treated similarly but more efficiently than under Basic Curtailment.

- **Smart Curtailment**: Smart curtailment, as defined in this paper, represents the optimal intervention of the DSO assuming perfect information and individual treatment of each charg-

ing process. With perfect information, the DSO is aware of EV users' economically optimal charging schedules and can calculate each household's time-dependent impact on grid elements. Based on this information, the DSO can forward individual and time-dependent curtailment factors to each household, effectively managing and optimizing charging processes within the grid.

By combining different tariff designs with various DSO intervention strategies, nine different use cases are formulated, as represented by the boxes in Figure 1. Additionally, a hypothetical case with no curtailment is considered a reference to illustrate potential bottlenecks that may occur before curtailment.

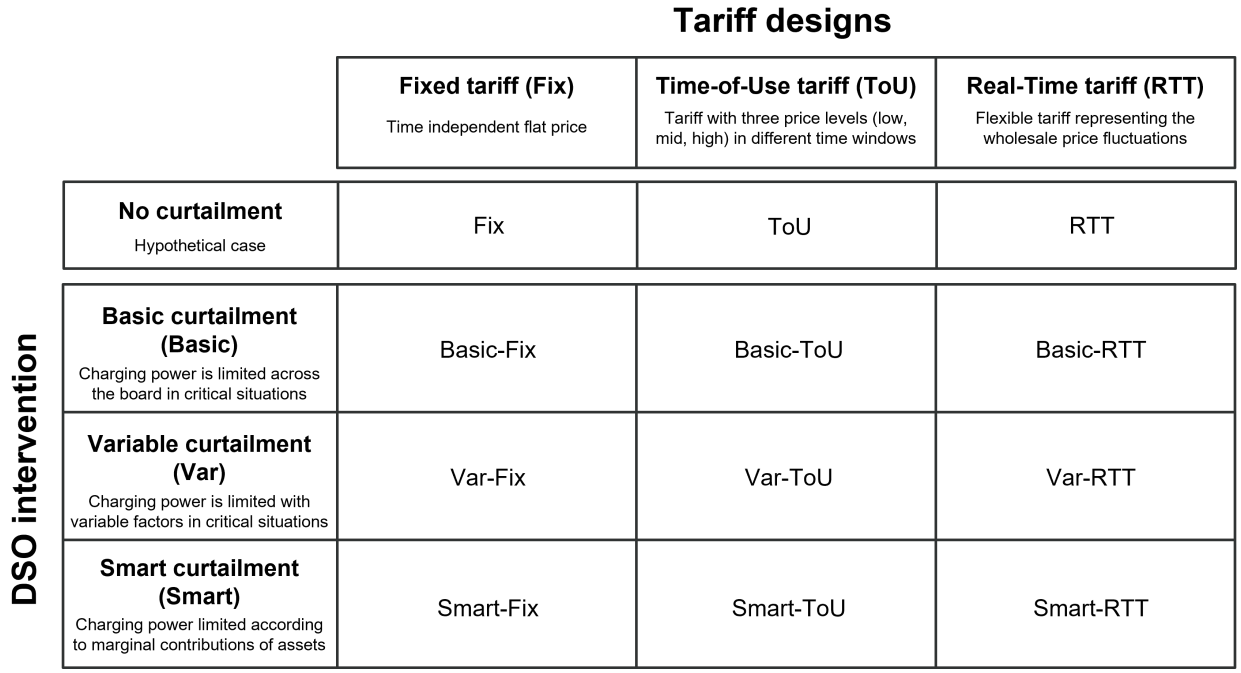

Figure 1: Combinations of electricity tariff designs and possibilities for interventions by the DSO

The figure illustrates how we label our different use cases. Each combination of DSO intervention and tariff design is labeled with an individual name.

Combining a specific tariff design with one possible intervention strategy reflects one setting for optimizing households and the related charging processes. Our model approach will be described in the following chapter.

3. Grid interventions in the context of optimizing charging processes

This chapter introduces a new model to analyze the effects of different electricity tariff designs combined with DSO intervention concepts on grid utilization and electricity costs. This model comprises two components: an asset optimization model to minimize households' electricity costs, explained in Section 3.1, and a grid model, introduced in Section 3.2. Information from the grid model regarding grid signals is considered in the optimization model with the help of load and generation distribution factors. These factors are considered using new equations within the optimization model. The methodology of this linkage, implemented in three different ways for the three intervention strategies, is explained in Section 3.3. Section 3.4 gives an overview of the process of calculations.

By considering signals from the grid within the central optimization, our holistic model provides a comprehensive perspective that incorporates the characteristics of the grid and the economic optimization of charging processes and their mutual dependencies. The approach allows us to maintain the computational efficiency of both the market and grid models. The modular nature of the model linkage with the distinction of controllable and non-controllable assets makes it applicable to individual distribution grid topologies and scenarios.

3.1. Optimization of decentralized energy systems

In this study, we develop a model for the economic analysis of decentralized energy systems. It is designed as a linear optimization program that maximizes individual entities' profits following a price-taking assumption and the assumption of perfect foresight. The operation of decentralized, controllable assets is optimized based on technical and economic parameters. The model also allows for analyzing the effects of fixed and variable retail tariffs.

The model can simultaneously optimize the electricity and heat turnover for multiple households in a distribution grid. The model comprises electricity-related consumption and production technologies with all relevant parameters, such as heat pumps, electric vehicles, storage units, and entities with heat and electricity demand. The model maximizes each household's profit while covering the heat and electricity demand. Depending on the setting, the required electricity for direct consumption

or heat production is either produced by the households' technologies, such as PV systems, or obtained from an electricity supplier. Maximizing the profits, thus, is equivalent to minimizing the cost of energy supply. Equation (1).

$$\max \sum_{q \in Q} [\sum_{c \in G_{el}} P_{c,q}^{g_{el},f} * m_c^f - \sum_{c \in L_{el}} P_{c,q}^{l_{el},p} * (p_q^w + t)] \tag{1}$$

The model optimizes the asset deployment for each time interval q. The first term of the objective function, for each generation unit c, represents the generated electricity in the interval q, which is fed into the grid and reimbursed by the feed-in tariff m_c^f. The second term represents electricity procurement for each electricity-consuming asset. The parameter p_q^w represents the provisioning component of the consumer price, while t comprises the taxes and levies.

The equations (2) until (5) are demand and supply equations for electricity (2, 3) and heat (4, 5). The equations break down energy generation and consumption to their purposes. The electricity generation $P_{c,q}^{g_{el}}$ splits into electricity fed into the grid ($P_{c,q}^{g_{el},f}$) and provided for electricity consumers $c' \in C$ on-site ($P_{c,c',q}^{g_{el}}$). The electricity consumption ($P_{c,q}^{l_{el}}$) in equation (3) splits correspondingly into electricity procured ($P_{c,q}^{l_{el},p}$) from an electricity provider, and the consumption covered by on-site generation units.

$$P_{c,q}^{g_{el}} = P_{c,q}^{g_{el},f} + \sum_{c' \in L_{el}} P_{c,c',q}^{g_{el}} \quad \forall q \in Q \wedge c \in G_{el} \tag{2}$$

$$P_{c,q}^{l_{el}} = P_{c,q}^{l_{el},p} + \sum_{c' \in G_{el}} P_{c,c',q}^{l_{el}} \quad \forall q \in Q \wedge c \in L_{el} \tag{3}$$

$$P_{c,q}^{g_{th}} = \sum_{c' \in L_{th}} P_{c,c',q}^{g_{th}} \quad \forall q \in Q \wedge c \in G_{th} \tag{4}$$

$$P_{c,q}^{l_{th}} = \sum_{c' \in G_{th}} P_{c,c',q}^{l_{th}} \quad \forall q \in Q \wedge c \in L_{th} \tag{5}$$

The equations (6) to (16) set the technical constraints for the considered technologies. Equation (6) limits the generation of electricity generators by their installed capacity i_c and the time-dependent

availability profile s_q. For intermittent resources like PV systems, s_q varies during the day based on the considered weather year.

$$P_{c,q}^{g_{el}} \leq \frac{1}{4} i_c * s_q \quad \forall q \in Q \wedge c \in G_{el} \tag{6}$$

Power-to-heat technologies, such as heat pumps and heating rods, are defined by equations (7) and (8) based on Frings and Helgeson (2022). The first equation determines the conversion of electricity into thermal energy ($P_{c,q}^{g_{th}}$). The conversion is based on the time- and asset-dependent efficiency $\eta_{c,q}^{el}$, including the COP. The latter equation restricts the electricity consumption $P_{c,q}^{l_{el}}$ based on the installed electric power.

$$P_{c,q}^{l_{el}} * \eta_{c,q}^{el} = P_{c,q}^{g_{th}} \quad \forall q \in Q \wedge c \in (L_{el} \cup G_{th}) \tag{7}$$

$$P_{c,q}^{l_{el}} \leq \frac{1}{4} i_c^{el} \quad \forall q \in Q \wedge c \in (L_{el} \cup G_{th}) \tag{8}$$

Finally, electric and thermal storage equations are defined in constraints (9) to (12). Equations (9) and (10) restrict the maximum state of charge (SOC) for thermal and electric storage units, including electric vehicles. Equations (11) and (12) limit the charging and discharging of storage units alike. The factor $d_{c,q}$ represents a storage's grid connection. For regular storage units, the grid connection is constantly given ($d_{c,q} = 1$). Electric vehicles, however, are disconnected from the grid during their trips ($d_{c,q} = 0$).

$$SOC_{c,q}^{el} \leq i_c^{soc,el} \quad \forall q \in Q \wedge c \in (L_{el} \cup G_{el}) \tag{9}$$

$$SOC_{c,q}^{th} \leq i_c^{soc,th} \quad \forall q \in Q \wedge c \in (L_{th} \cup G_{th}) \tag{10}$$

$$P_{c,q}^{g_{el}} \leq P_{c,q}^{l_{el}} \leq \frac{1}{4} i_c^{el} * d_{c,q} \quad \forall q \in Q \wedge c \in (L_{el} \cup G_{el}) \tag{11}$$

$$P_{c,q}^{g_{th}} \leq P_{c,q}^{l_{th}} \leq \frac{1}{4} i_c^{th} * d_{c,q} \quad \forall q \in Q \wedge c \in (L_{th} \cup G_{th}) \tag{12}$$

For storage units, the continuity and the balancing constraints are shown in equations (13) to (16). In the first equation, the SOC is determined by the SOC of the previous interval, the charged and discharged energy. Electric vehicles' electricity consumed in trips is removed once at departure. It is included in addend $r_{c,q}$. η represents the charging and discharging efficiency. The balancing

equation (15) ensures that, at large, demand and supply are balanced, including the consumption by trips for electric vehicles.

$$SOC^{el}_{c,q} = SOC^{el}_{c,q-1} + P^{l_{el}}_{c,q} * \eta^{el}_{c,q} - \frac{P^{g_{el}}_{c,q}}{\eta^{el}_{c,q}} - r_{c,q} \quad \forall q \in Q \wedge c \in (L_{el} \cup G_{el}) \tag{13}$$

$$SOC^{th}_{c,q} = SOC^{th}_{c,q-1} + P^{l_{th}}_{c,q} * \eta^{th}_{c,q} - \frac{P^{g_{th}}_{c,q}}{\eta^{th}_{c,q}} \quad \forall q \in Q \wedge c \in (L_{th} \cup G_{th}) \tag{14}$$

$$\sum_{q \in Q} \frac{P^{g_{el}}_{c,q}}{\eta^{el}_{c,q}} + r_{c,q} = \sum_{q \in Q} (P^{l_{el}}_{c,q} * \eta^{el}_{c,q}) \quad \forall c \in (L_{el} \cup G_{el}) \tag{15}$$

$$\sum_{q \in Q} \frac{P^{g_{th}}_{c,q}}{\eta^{th}_{c,q}} = \sum_{q \in Q} (P^{l_{th}}_{c,q} * \eta^{th}_{c,q}) \quad \forall c \in (L_{th} \cup G_{th}) \tag{16}$$

Given the explained model, various operating schemes are deployed and used to analyze the different combinations of tariffs and DSO interventions explained in chapter 2. The different electricity tariffs are modeled by parameterizing p^w_q. For the fixed tariff, the parameter is constant for all time intervals, while for the time-of-use tariff, it is piece-wise constant in different time windows. For modeling the real-time tariff, the parameter is fully flexible in each time interval.

3.2. Grid model

The optimization model initially determines the operational strategy for the assets without considering potential grid constraints. Therefore, we perform an AC power flow to check whether the computed solution is physically feasible. If bottleneck situations occur, assets affecting congestion have to change their load or supply. Consequently, the impact of single assets on the power flow of specific lines and transformers has to be determined. Generation and load distribution factors provide information about the contribution of single assets to the total flow on a line. With the help of those distribution factors and the information on maximum line utilization, new constraints in the optimization model prevent bottlenecks in the distribution grid during asset optimization. Based on the optimization results, the AC power flow uses the time series of each asset located in the distribution grid as input. Market results only contain information on active power dispatch, so the reactive power is calculated afterward. Based on Dynge et al. (2021), we assume a fixed power

factor of $\cos(\varphi)$ equal to 0.98 for all loads. Reactive power is calculated as given in equation (17). Batteries and generators do not provide or consume reactive power.

$$Q = \sqrt{\frac{P^2}{\cos(\varphi)^2} - P^2} = \sqrt{\frac{1}{\cos(\varphi)^2} - 1} * P = k * P \tag{17}$$

The AC power flow is performed with each asset's active and reactive power time series input. The results, such as line loading and line flows, are then used as necessary inputs for matrix operations according to Schneider et al. (2018) and Kłos et al. (2015). By applying their presented methods, the contribution of single assets on the line loading can be obtained. The most important steps to obtain the distribution factors are described in the following paragraphs.

The total flow P $(Nx1)$ is calculated using either an upstream or a downstream approach based on power flow results. The upstream approach considers all feeding flows, while the downstream approach accounts for all draining flows of a given node. Following the upstream approach, an element F^{in}_{nm} of F^{in} contains the power injected at the node m if a line between n and m exists. Otherwise, the entry is zero. Additionally, the nodal generation p^g_n is added. On the other hand, the downstream approach accumulates all flows draining node n and the nodal load p^l_m.

$$P = \begin{pmatrix} P_n \\ \vdots \\ P_N \end{pmatrix} \quad \text{with } P_n = \sum_{n \in N} F^{in}_{n,m} + P^g_n = \sum_{m \in N} F^{out}_{n,m} + P^l_m \tag{18}$$

Virtual nodes with generation or supply equal to the line loss are added at the middle of each line. The line is then split into two parts. Both are then without losses.

Next, the matrices of flow contribution C (NxN) and flow distribution A (NxN) are computed as shown in equations (19) to (22), I describing the identity matrix.

$$C_u = diag^{-1}(P) * F^{in} \tag{19}$$

$$A_u = I - C_u^T \tag{20}$$

$$C_d = F^{out} * diag^{-1}(P) \tag{21}$$

$$A_d = I - C_d \tag{22}$$

The matrices C and A can be used to obtain generation distribution factors GDF (MxN) and load distribution factors LDF (MxN).

$$GDF = diag(\Lambda(G_f C_u C_t^T))G_f A_u^{-1} \tag{23}$$

$$LDF = diag(\Lambda(G_f C_d C_t^T))G_f A_d^{-1} \tag{24}$$

The Λ operator returns the diagonal elements of a square matrix. G_f (NxM) represents the incidence matrix with 'from'-nodes and G_t (NxM) is the incidence matrix with 'to'-nodes. The element $gdf_{k,m}$ indicates the share of injected power at node m flowing on line k. Likewise, $ldf_{k,m}$ indicates the share of withdrawn power at node m flowing on line k. With the distribution factors, new equations in the market model are formulated, as described in the next subsection.

3.3. Coupling of the asset optimization model and grid model

The way distribution factors are used to formulate new constraints in the asset optimization model reflecting line and transformer capacity limits depends on the type of grid signal associated with the curtailment approach. As presented in chapter 2, three types of grid signals are considered. In the case of basic curtailment, the maximum load of each electric vehicle behind a bottleneck is limited during a specific time interval. Variable curtailment reflects curtailing all electric vehicles behind a bottleneck with the same time-dependent curtailment factor. In the case of smart curtailment, single EVs are individually controlled optimally to resolve congestion, assuming perfect information.

Basic Curtailment: Equation (25) is used for the basic curtailment concept. Only information about congested lines and transformers is considered in the LDF matrix. Consequently, values larger than 0 reflect a contribution of node n to the power flow on a congested line or transformer k. Transferred into reality, LDF is a model-based approximation of the information regarding congestions and affected nodes behind that bottleneck. If a node with an EV contributes to congestion, the maximum charging power i_c^{el} is multiplied by $0 < e < 1$. α_c is a set of nodes connected to a

component c. The value of e depends on the penetration rate for EVs and represents a curtailment factor determined a priori. All EVs behind a bottleneck face the same curtailment.

$$\frac{4}{h} * P_{c,q}^{l_{el}} \leq \begin{cases} i_c^{el} * e & \text{,if } \sum_{k \in K} \sum_{n \in \alpha_c} ldf_{k,n,q} > 0 \\ i_c^{el} * 1.0 & \text{,if } \sum_{k \in K} \sum_{n \in \alpha_c} ldf_{k,n,q} = 0 \end{cases} \quad \forall q \in Q \wedge c \in L_{el} \tag{25}$$

Variable Curtailment: Variable curtailment builds upon the principles of Basic Curtailment but incorporates additional information concerning the actual load and congestion levels. Instead of applying a fixed curtailment factor to all EVs located behind a bottleneck, time-dependent signals are transmitted to them. Although all EVs behind the bottleneck experience the same level of curtailment, the intensity varies over time, aligning with the real-time utilization patterns. Equation (26) can be formulated based on these assumptions.

$$\frac{4}{h} * P_{c,q}^{l_{el}} \leq \begin{cases} i_c^{el} * e_{c,q} & \text{,if } \sum_{k \in K} \sum_{n \in \alpha_c} ldf_{k,n,q} > 0 \\ i_c^{el} * 1.0 & \text{,if } \sum_{k \in K} \sum_{n \in \alpha_c} ldf_{k,n,q} = 0 \end{cases} \quad \forall q \in Q \wedge c \in L_{el} \tag{26}$$

Smart Curtailment: For modeling smart curtailment, two more advanced equations are used instead of equation (25) or (26) to consider optimally determined grid signals within the optimization model to prevent grid congestions. To achieve this, we assume perfect information regarding grid utilization, the impact of single nodes on power flow, and the possibility of controlling each electric vehicle individually. Assuming that only a fraction of the assets in the distribution grid is controllable, GDF and LDF only include the contribution values of the respective nodes. Consequently, for all transformers and loads, we differentiate between the total maximum capacity limit $P_{k,q}^{max}$ and the maximum capacity limit $P_{k,q}^{max,controllable}$ related to the nodes with controllable assets. Figure 2 visualizes this relationship. For simplicity, S, P, and Q reflect power values with no temporal and spatial component.

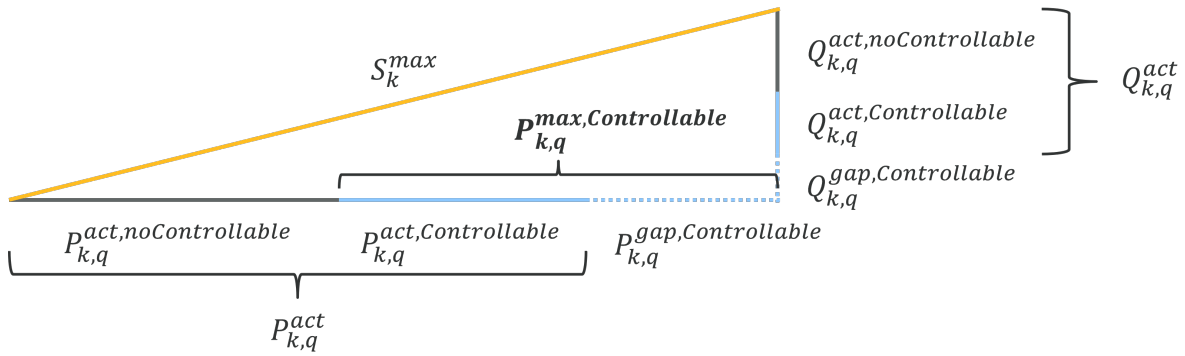

Figure 2: PQ-Diagram to determine the maximum, controllable active power on grid elements

The capacity limit of each line or transformer k is defined by the maximum apparent power S_k^{max}. The apparent power consists of an active and reactive part. Each part can be further decomposed into three parts. The first part ($P_{k,q}^{act,noControllable}$ and $Q_{k,q}^{act,noControllable}$) respectively includes the contribution of all nodes in a specific time interval q on line and transformer flow that have no controllable assets. A second part ($P_{k,q}^{act,Controllable}$ and $Q_{k,q}^{act,Controllable}$) includes the actual contribution of all nodes on line and transformer flow which have controllable assets such as electric vehicles. The last part ($Q_{k,q}^{gap,Controllable}$ and $Q_{k,q}^{gap,Controllable}$) defines a gap that reflects the maximum additional active and reactive power on a line or transformer until the maximum apparent power is reached. In case the maximum apparent power is already reached by the actual active ($P_{k,q}^{act}$) and reactive power ($Q_{k,q}^{act}$), this gap has to be negative. Dispatch of the different controllable assets has to be readjusted to stay within the maximum apparent power. In the market model, only $P_{k,q}^{max,Controllable}$ is used, which corresponds to $i_{k,q}^{max}$ there. Appendix A describes its calculation in detail.

With the values for LDF, GDF and $i_{k,q}^{max}$, equations (27) and (28) can be formulated in the optimization model. Equation (27) considers all controllable nodes with generation larger than load (generation nodes), and equation (28) does the same for all controllable load nodes.

$$\frac{4}{h} * \sum_{n \in N} [max(0_{n,q}, \sum_{c \in \alpha_n} P_{c,q}^{g_{el}} - \sum_{c \in \alpha_n} P_{c,q}^{l_{el}}) * gdf_{k,n,q}] \leq i_{k,q}^{max} \quad \forall k \in K \wedge q \in Q \tag{27}$$

$$\frac{4}{h} * \sum_{n \in N} [max(0_{n,q}, \sum_{c \in \alpha_n} P_{c,q}^{l_{el}} - \sum_{c \in \alpha_n} P_{c,q}^{g_{el}}) * ldf_{k,n,q}] \leq i_{k,q}^{max} \quad \forall k \in K \wedge q \in Q \tag{28}$$

Components are mapped to the respective node with the matching set α_n, and the balance is calculated. From the generation perspective, by multiplying the nodal generation ($\sum_{c\in\alpha_n} P_{c,q}^{g_{el}} - \sum_{c\in\alpha_n} P_{c,q}^{l_{el}}$) with the GDF matrix, the power flow on each line caused by the respective node is computed. After summing over all nodes, the total power flow on each line or transformer k is the result. For all lines and transformers in the system, the total power flow has to be lower than the maximum capacity limit $i_{k,q}^{max}$. The same can be formulated for nodes treated as load nodes, as done in equation (28).

3.4. Process of calculations

Figure 3 shows how the optimization and grid model interact in an iterative process to quantify the effects of different tariff structures and intervention options of the DSO. The process slightly differs between basic, variable, and smart curtailment. The columns relate to different simulation or optimization steps.

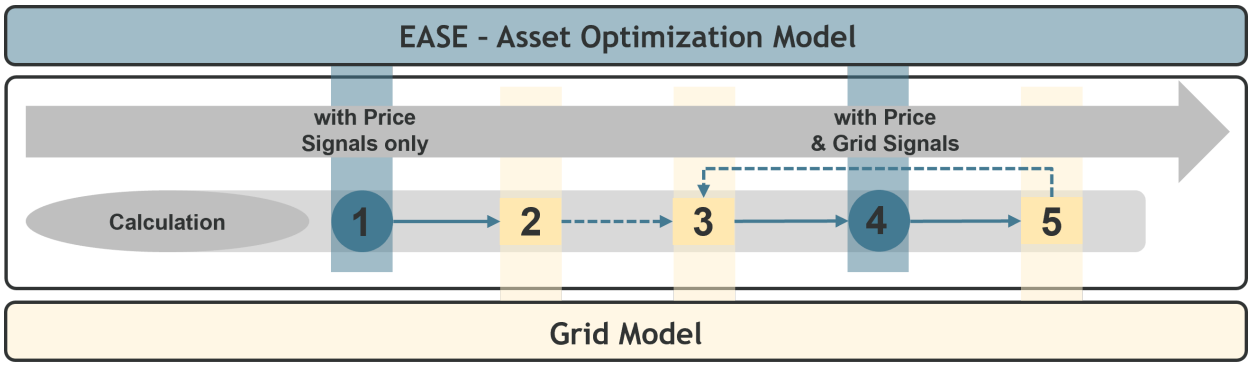

Figure 3: Process diagram illustrating the various optimization and computation steps

In the **first step**, the simulation and optimization of all decentralized assets and households are done by running the optimization model without considering the grid. Fixed, ToU or Real-Time prices are used depending on the selected tariff design. One of the results is the optimal charging strategy for each household. In the **second step**, an AC power flow is performed to check the validity of the optimization results. If there is no congestion, the model will stop here. In the case of line or transformer overloading, the **third step** follows. Here, the necessary parameters are calculated to consider the grid situation within the optimization model. The method of calcu-

lation varies according to the curtailment strategy. Regarding basic and variable curtailment, the generation and load distribution factors are calculated only for the respective time intervals and congested elements. In the case of smart curtailment, the generation and load distribution factors are calculated for all time intervals and grid elements together with the line and transformer capacity limits. Depending on the curtailment strategy, the respective constraints are parameterized and used in the optimization model to reflect the signals from the grid, as described in section 3.3. Then, the optimization model is rerun in the **fourth step**, considering the additional constraints depending on the curtailment strategy. These new constraints reflect the signals from the grid. The validity of the asset operations concerning potential grid constraints is checked again in the final **fifth step**. If there is no congestion remaining, the process stops after step five. But, in the case of basic and variable curtailment, new congestion can occur by shifting the load to time intervals when charging power is not limited. Consequently, these additional time intervals must then be considered additionally. This is done by rerunning step 3 and updating the matrices with generation and load distribution factors. In the case of variable curtailment, the curtailment factor $e_{c,q}$ is increased marginally when necessary. In the case of smart curtailment, the process ends here, except that the nodal balance of individual nodes within the distribution system after step four changes the sign from the result after step one. [2]

4. Case Study - Technical and economic effects of different intervention concepts

We employ the formulated model alongside the proposed combinations of tariff schemes and diverse intervention methods by the DSO to a synthetic distribution grid represented as a case study. Within this chapter, we focus on optimal EV charging strategies in combination with various electricity tariff schemes and examine the implications of distinct DSO intervention methods. The computed outcomes cater to a range of EV penetration rates. Section 4.1 details the case study's context and base data. Section 4.2 explores the first research question addressing the impact of dis-

[2] Nodal balance could switch from positive to negative or the other way round after one iteration. For example, a load node could become a generation node if PV generation remains high and the load is curtailed and shifted to other time intervals. Then, the generation and load distribution factors are calculated again in step three for all time intervals and nodes. The highest values from the first and second iterations determine the new matrices.

parate tariff structures on optimal EV charging strategies and, subsequently, grid utilization under various EV penetration rates. Section 4.3 is devoted to the second research question, focusing on the implications of the DSO's varied intervention concepts on optimal charging strategies, accounting for differing penetration rates. We analyze the impacts considering factors such as flexibility demand (Chapter 4.3.1) and charging costs (Chapter 4.3.2).

4.1. Analysis Environment

We parameterize the optimization model and a synthetic distribution grid to analyze the interdependencies of various tariff designs and DSO interventions. In the following section, we provide details regarding the grid configuration, the profiles used (including renewables, electricity prices, and charging profiles), the factors for curtailment (see chapter 3.2), and the considered period in the form of type days.

The analysis is based on the grid configuration "1-MVLV-semiurb-all-0-sw" made available by the SimBench project (Meinecke et al., 2020). The grid comprises 115 medium-voltage nodes with downstream low-voltage grids, as illustrated in Figure 4. However, only 12 connected low-voltage grids, consisting of 1015 low-voltage nodes, are explicitly modeled. In contrast, the remaining 103 low-voltage grids are aggregated with a predefined load pattern at their respective medium-voltage node.

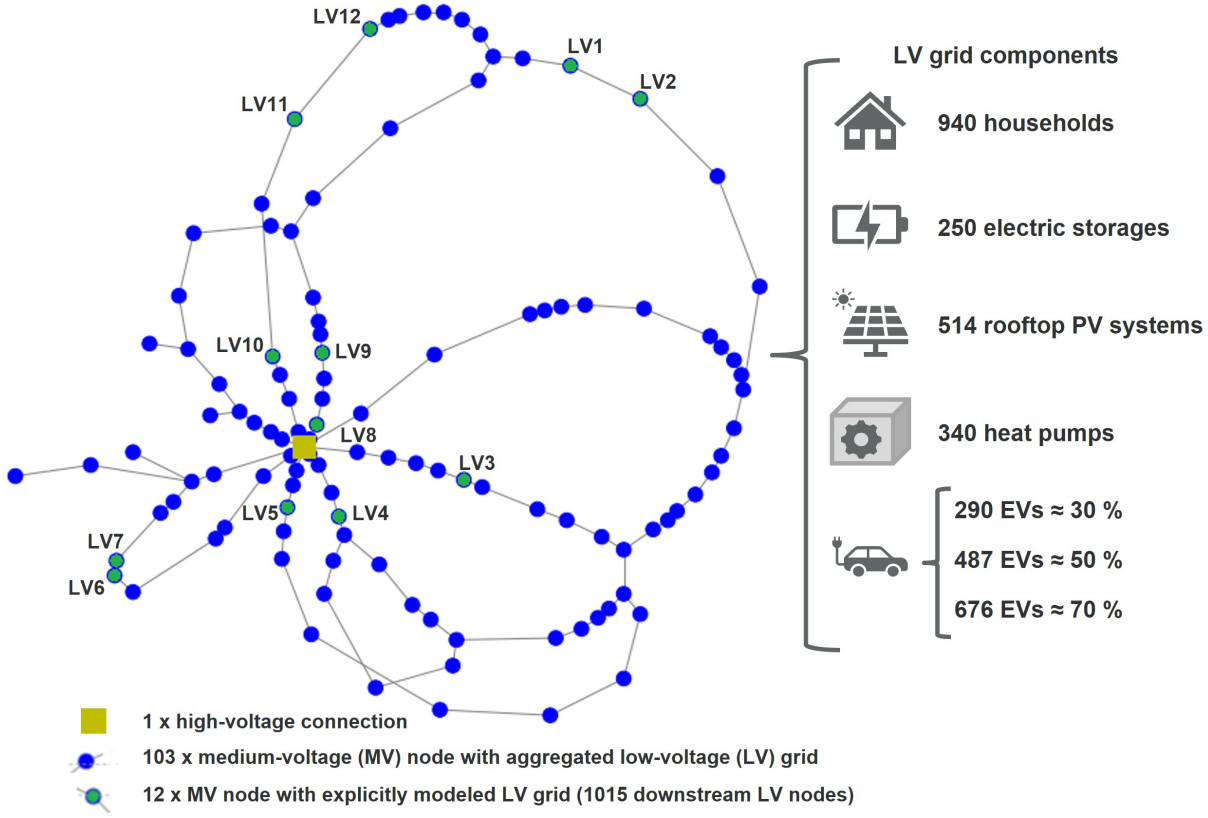

Figure 4: Configuration of the distribution grid

The analysis encompasses various distributed energy resources, including power-to-heat, photovoltaic (PV) systems, energy storage systems, and electric vehicles (EVs). For 2030, EV penetration rates for Germany are considered based on Hecking et al. (2018) and randomly allocated.

We model 940 households at individual nodes within the 12 low-voltage grids of different sizes. These low-voltage grids are assumed to represent relatively homogenous settlements with single-family houses. The base demand of households, excluding EVs and electric heating, is generated using a publicly available load profile generator (Pflugradt et al., 2022). In line with Birk et al. (2021), the profiles differ regarding the number of persons per household (two or four), efficiency levels, the number of gainfully employed persons, and vacation behavior, resulting in sixteen different types of households. Only households with an EV are considered controllable, as detailed in Chapter 3. The baseline configuration assumes an EV penetration rate of 30%, representing the proportion of households within the grid area possessing both an EV and a charging station. Scaling this

proportion would lead to approximately 14 million EVs in Germany KBA (2023). In addition to this baseline rate, the analysis also considers increased EV penetration rates of 50% and 70%. Within individual low-voltage grids, the EV penetration rates fluctuate between 23% and 68% for the baseline rate of 30%, reflecting variations in neighborhood affluence. Corresponding rates for EV penetration rates of 50% and 70% range from 41% to 79% and 65% to 100%, respectively. For the 12 low-voltage grids included in this study, the total energy consumption, inclusive of EVs, equals 7.3 GWh/a for the baseline EV penetration rate of 30%, 8.7 GWh/a for 40%, and 10.7 GWh/a for 50%. Additional details regarding the properties of the modeled 12 low-voltage grids can be found in Appendix B.

Renewable generation profiles are determined based on the weather year 2015 and a representative weather station in North Rhine-Westphalia, Germany. For modeling the retail prices, we adjust the procurement component of the consumer prices for the different tariffs based on expected day-ahead wholesale prices based on the future energy system scenario "EL80" from Hecking et al. (2018) using the energy system model DIMENSION (Helgeson and Peter, 2020). All components of the consumer price, such as the grid usage fees, levies, and electricity tax, are taken from the selected scenario and consistently applied across all tariffs. The value-added tax of 19% is subsequently calculated based on the consumer price components. We disregard the retailer's added margin and distribution components to streamline the model. The distribution component includes a risk premium depending on the respective tariff. As the dynamics of the tariffs increase, the risk premium reduces due to price risks being transferred to consumers. The risk premium is virtually zero for fully dynamic tariffs. The distribution of the resulting wholesale prices and the derived average consumer prices for both the Fixed tariff and the Time-of-Use tariff can be seen in Figure 5. The 2030 quarter-hourly wholesale prices on the left fluctuate around 59.6 EUR/MWh with an average peak price of about 62.3 EUR/MWh.

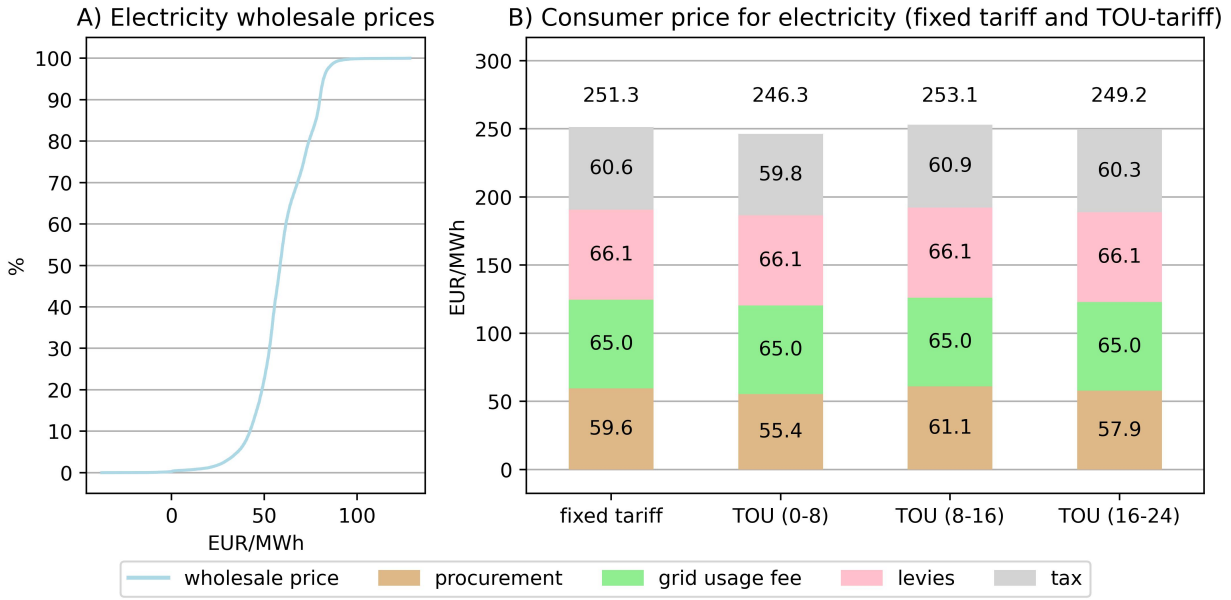

Figure 5: Electricity prices: A) Cumulated distribution of assumed electricity wholesale prices (2030) B) Composition of the electricity price for consumers (2030)

For each type day, consisting of three consecutive days, we define the Fixed and the TOU tariff based on the respective wholesale prices individually to ensure comparability of prices. On average, the procurement component for the Fixed tariff corresponds to the average wholesale price of 59.6 EUR/MWh, culminating in an average total fixed consumer price of 251.3 EUR/MWh. The Time-of-Use tariff features three price levels that apply regardless of the type of day (weekends or weekdays). The procurement components mirror the average annual prices within three time windows. On average, the tariff structure encourages charging in the first third of the day (246.3 EUR/MWh) over the last third (249.2 EUR/MWh), with charging in the second third of the day being the least favored (253.1 EUR/MWh). For the Real-Time tariff, the procurement component of the consumer prices equals the quarter-hourly wholesale price. For the year under consideration, the prices vary between -33.2 and 475.7 EUR/MWh, with the average price aligning with the fixed consumer price. The characteristics of the EVs are summarized in figure 6. The left side shows the cumulative distribution of daily energy consumption, with a mean value of about 11 kWh daily. The EV users, thus, represent frequent commuters. The right side shows the share of EVs connected to the grid during three representative days. It shows a typical commuting pattern. At noon,

EVs are not at home and, thus, not connected to the grid, while they are at night. The electric vehicles are charged up to a maximum capacity of 11 kW. EVs can be charged anything between sufficiently charged for the next trip and until the batteries are fully charged. EVs are connected to the charging station when they arrive home, even though the charging processes do not necessarily start immediately. Additionally, maximizing the self-consumption, i.e., if a PV system is available, is a fundamental consumption strategy that also affects the charging behavior.

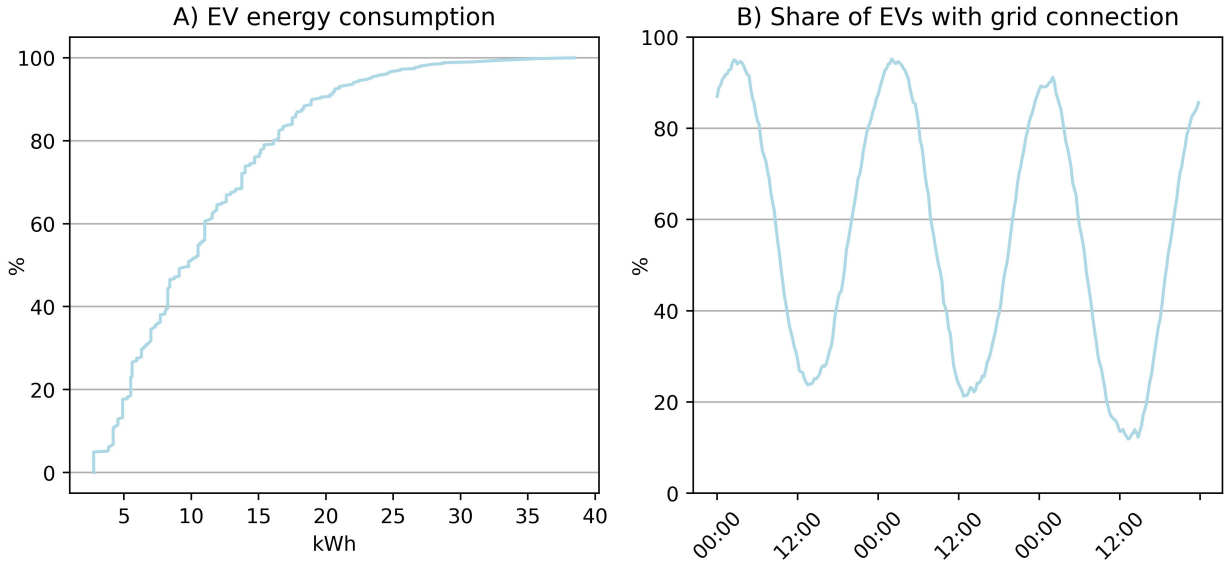

Figure 6: A) Cumulated distribution of EVs' daily energy consumption and B) Share of EVs with grid connection over time

Depending on the penetration rate and the tariff design, the curtailment factor for basic curtailment (e) (see equation (25)) is varied according to the table 1. Each factor is used for the whole distribution grid. The variation is necessary because the need for curtailment increases with higher penetration rates and more dynamic electricity tariffs.

Table 1: EV curtailment in use cases with basic curtailment

Concept	**EV penetration 30 %**	**EV penetration 50 %**	**EV penetration 70 %**
Basic-Fix	0 %	0 %	20 %
Basic-ToU	35 %	60 %	75 %
Basic-RTT	35 %	60 %	75 %

For performance reasons, the year under consideration is divided into 16 typical days to reduce the computation time. The 16 days correspond to eight winter and eight summer days, as well as

eight working days and eight weekend days. The days are weighted individually and add up to 365 days. To analyze storage operation for more than one day, the preceding and following days for each typical day are included in the calculations. A detailed description is given in Birk et al. (2021) regarding the production and consumption profiles for the considered assets.

4.2. Impact of different tariff structures on optimal charging strategies and grid utilization

This section investigates how tariff structures alter EV charging strategies and consequently impact grid utilization. Initially, we scrutinize load pattern variations specific to an individual transformer and a three-day time interval across different tariff schemes. This analysis is conducted for the three EV penetration rates, denoted as 'dRates'. Additionally, we calculate changes in absolute electricity costs for each tariff design and penetration rate. We use the costs associated with the fixed-tariff scheme as a benchmark, enabling a standardized comparison of tariff cost-effectiveness and highlighting the economic implications of different tariff structures for EV charging. The results of this analysis are illustrated in Figure 7, divided into two parts. The left-hand side demonstrates the demand profile, visualizing how EV charging demands fluctuate under various tariff structures and penetration rates. Conversely, the right-hand side represents absolute electricity costs.

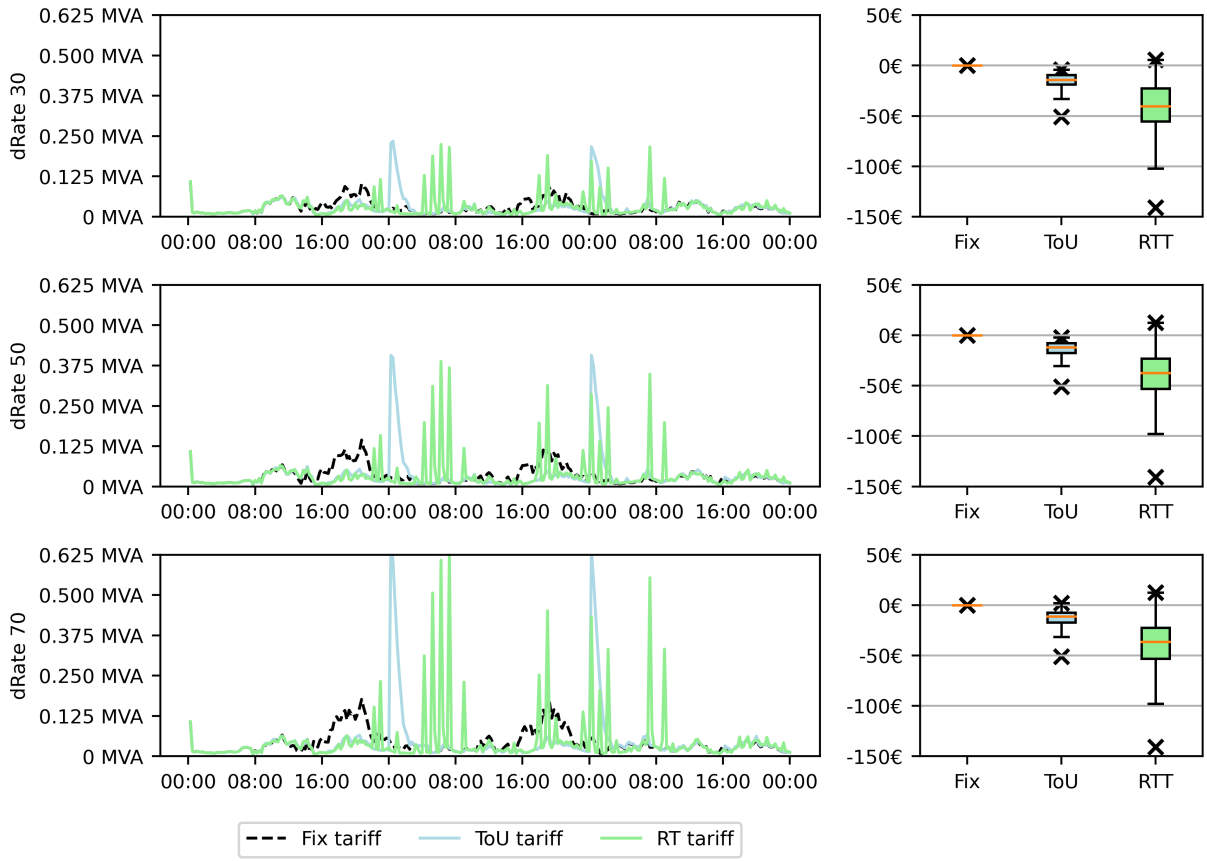

Figure 7: Impact of tariff structures on optimal charging strategies and related charging costs without curtailment

Note: The left segment of the figure concretely portrays the demand patterns tied to a singular transformer for three days. The distribution of charging costs depicted on the right is calculated annually, encompassing all vehicles distributed across the twelve grids. Each row reflects the results for a given penetration rate.

Examining variations in total electricity costs for individual electric vehicles reveals interesting trends. Notably, the implementation of dynamic tariffs results in a reduction in total costs for almost all households when compared to the Fixed tariff. Among the dynamic tariff structures, Real-Time Pricing emerges as particularly influential, outweighing the impact of Time-of-Use tariffs. With the ToU tariff, households experience weighted average savings of 16.9 EUR across all penetration rates. At the same time, a stronger trend is observed with the RT tariff, where households save an average of 47.2 EUR across all penetration rates. Only a few households experience increasing electricity costs, driven by individual charging patterns correlated with high-price windows. However, when compared to the total electricity expenses of each household, the changes in costs are relatively small.

Specifically, the Time-of-Use tariff decreases relative electricity costs by about 1.0%, whereas the Real-Time tariff yields slightly higher savings of about 3%.

The observed fluctuations in charging costs can be attributed to the shifting demand in response to price signals. In the case of the ToU tariff, we observe demand being diverted primarily towards the early hours of the day, between 00:00 and 09:00. This shift is driven by the lower electricity prices prevalent during this time window. Conversely, under the RTT scheme, the charging mechanisms are more reactive to granular, 15-minute price signals, with the demand being lowest during the night.

When considering all tariff schemes, it's important to understand that adjusting optimal charging strategies and increasing the penetration rate of EVS could potentially lead to congestion in the distribution feeders. The provided table 2 analyses potential transformer overloads in the twelve Low Voltage grids, given different EV penetration rates and under various electricity tariff schemes.

Table 2: Number of events of potential transformer overloadings

	dRate 30			**dRate 50**			**dRate 70**		
Grid	**Fix**	**ToU**	**RTT**	**Fix**	**ToU**	**RTT**	**Fix**	**ToU**	**RTT**
LV1	0	0	0	0	0	0	0	0	0
LV2	0	378	220	0	1014	982	41	1272	1387
LV3	0	303	180	0	920	1000	59	1218	1437
LV4	0	0	0	0	933	859	0	1077	1098
LV5	0	278	106	0	664	618	0	957	951
LV6	0	319	185	0	603	625	0	898	960
LV7	0	79	48	0	647	632	0	937	1005
LV8	0	0	0	0	23	0	0	27	19
LV9	0	0	0	0	0	0	0	0	0
LV10	0	0	0	0	0	0	0	47	17
LV11	0	0	0	0	26	20	0	497	383
LV12	0	0	6	0	0	0	0	96	43
Total	0	1357	739	0	4830	4736	100	7026	7300

Note: The number of events in each distribution grid refers to a whole year with a maximum of 35040 time steps. The total value is the sum over all events in one column.

The absence of overload events in grids LV1, LV8, LV9, and LV10, across all scenarios, indicates the resilience of these grids to increased EV penetration and tariff variations. On the other hand, for grids like LV2, LV4, LV6, and LV7, the number of overload events tends to increase with the EV penetration rate and varies significantly between tariff schemes. The RTT scheme shows increased

susceptibility to overloads as the EV penetration rate rises. This suggests that while RTT schemes may offer real-time pricing benefits, they could lead to potential grid congestion when not adequately managed, particularly in scenarios of high EV penetration. The ToU tariff scheme exhibits a moderate number of overload events in the scenario with a low penetration rate, suggesting a balanced approach, but records a significant rise in potential overloads as EV penetration rates increase. The results stress the vital role that DSOs must play in ensuring the stability of the power grid. Interventions by DSOs become crucial to prevent potential transformer overloads and maintain the grid's reliability and resilience in the case penetration rates increase and dynamic electricity tariffs are introduced. The effects of different DSO intervention strategies are evaluated in the following two sections.

4.3. Impact of different intervention options of the grid operator on optimal charging strategies

In this section, we address the second research question of quantifying the impact of different intervention options of the grid operator on optimal charging strategies. We do so by focusing on flexibility demand to avoid grid congestion (Subsection 4.3.1) and the change of charging costs in Subsection 4.3.2.

4.3.1. Flexibility provision in the whole grid area

The congestion on transformers and lines in the distribution grid is mitigated by flexible EV charging, as charging is shifted to other time intervals. The amount of shifted energy can be interpreted as a flexibility provision. Its value is calculated as the positive delta between the charging power of each electric vehicle before and after the grid signals as described in equation (29).

$$Flex = \sum_{EV} \sum_{t} [\max(i_{EV,t}^{before} - i_{EV,t}^{after}, 0)] \tag{29}$$

The amount of provided flexibility by electric vehicles to avoid congestion is visualized in Figure 8.

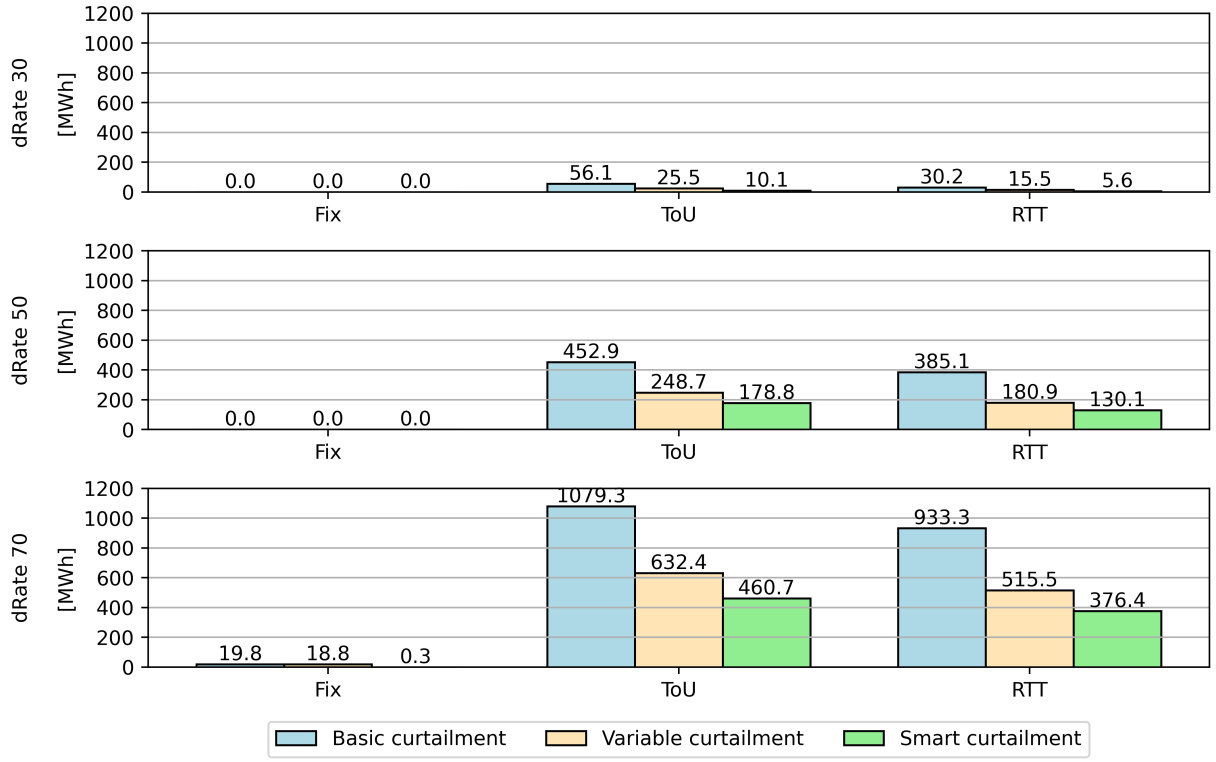

Figure 8: Flexibility provision by electric vehicles

The figure above shows a significant trend: introducing time-varying tariffs, such as Time-of-Use and Real-Time tariffs, directly correlates with increased flexibility demand to avoid congestion. When considering a 30% or even a 50% EV penetration rate, curtailment is not required under Fixed tariffs but becomes necessary as dynamic tariffs are introduced. The magnitude of the increase in flexibility demand due to the implementation of dynamic tariffs is not constant but depends on the electric vehicle penetration rate. Specifically, it is observed that with increasing EV penetration rates, the necessity for flexibility increases across all electricity pricing schemes and both curtailment strategies. For example, in the case of the ToU tariff combined with basic curtailment, the flexibility demand increases eightfold when comparing the results for a penetration rate of 30% with those for a rate of 50%. The demand reaches even more than 1000 MWh with basic curtailment if a penetration rate of 70% is assumed. Upon reaching the maximum analyzed penetration rate of 70%, the demand for flexibility experiences a substantial surge across all electricity pricing schemes and curtailment strategies. With increasing EV penetration rates, curtailment becomes indispensable

even for Fixed tariffs. Regarding the effectiveness of curtailment strategies, smart curtailment, the optimal benchmark, requires uniformly less flexibility than basic and variable curtailment across all pricing schemes, regardless of the EV penetration rate. Furthermore, variable curtailment always outweighs basic curtailment. This steady advantage highlights how a spatial and temporal differentiation of curtailment reduces the amount of flexibility and thus can help integrate more EVs into the electricity grid more easily. However, even in challenging scenarios, smart curtailment maintains its superiority over basic and variable curtailment, exemplifying its robustness and efficiency.

4.3.2. Electricity Costs

Figure 9 illustrates a comparative analysis of the annual variations in electricity costs, considering the TOU and RT tariffs, EV penetration, and the three different curtailment strategies. The comparison is made to the scenario featuring a fixed tariff without curtailment. Notably, the cost differentials for the fixed tariff are not visualized, as this tariff structure entails consistent costs irrespective of the employed curtailment approach.

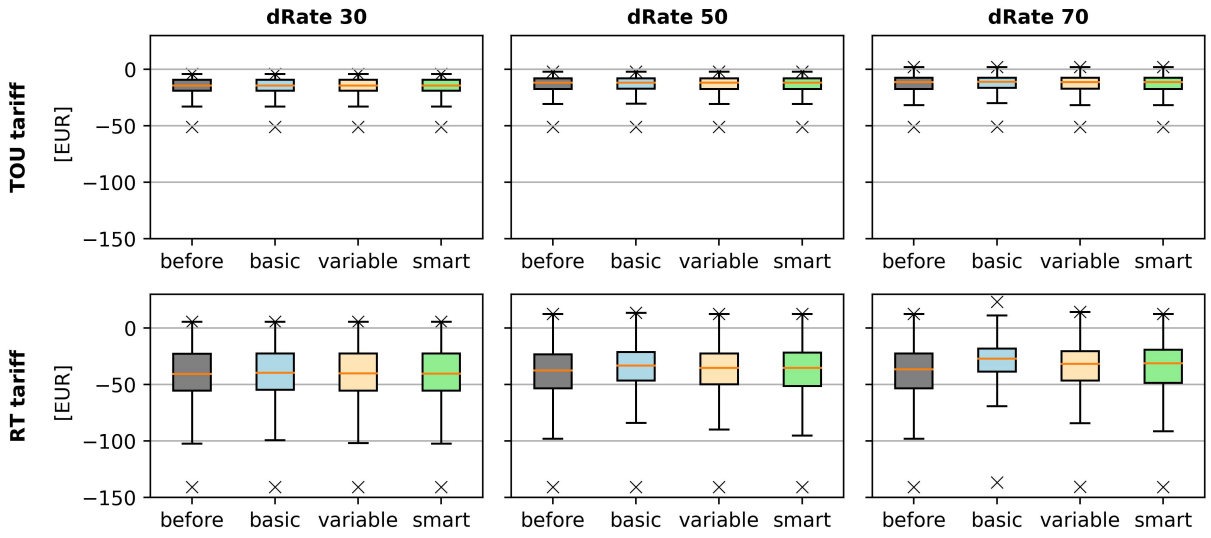

Figure 9: Comparison of cost deltas

Note: 'before' refers to the hypothetical case of charging exclusively based on price signals before curtailment strategies are deployed.

The boxplots depict that both TOU and RT tariffs exhibit reduced overall electricity costs for most households with flexible charging, both before and after the application of curtailment. However,

a minor increase in costs is observed for some households under variable tariffs. This is attributed to the limited flexibility of charging demand coincidentally aligning with higher electricity prices. Furthermore, on average, the RT tariff demonstrates an approximately threefold higher cost reduction than the TOU tariff. However, it is essential to note that the weighted average cost reductions compared to the fixed tariff are modest — around 1% for the TOU tariff and approximately 3% for the RT tariff. This is due to the variable component constituting only a minor fraction of the retail price. The cost delta for the TOU tariff appears almost independent of the curtailment strategy, as the deltas remain unchanged compared to the scenario before curtailment. This can be attributed to the length of the chosen TOU tariff intervals, which allows for sufficient load shifting to meet the grid limitations at the same price level.

In contrast, for the RT tariff, the curtailment strategy impacts the cost delta, which depends on the EV penetration rate. While curtailment has a marginal impact on cost deltas at an EV penetration rate of 30%, its effects become more pronounced at rates of 50% and 70%. Comparing these scenarios to cases without curtailment, basic curtailment, the least efficient concept, diminishes cost savings more significantly than variable and smart curtailment. This effect intensifies with an increasing EV penetration rate, necessitating more substantial load shifting to comply with grid constraints.

At an EV penetration rate of 50%, the weighted average cost delta under basic curtailment decreases by approximately 4.7 EUR compared to the scenario without curtailment. Variable and smart curtailment exhibit a milder reduction by 2.2 EUR and 1.4 EUR, respectively. Consequently, the cost savings under variable curtailment closely align with those achieved through smart curtailment.

For an EV penetration of 70%, the weighted average cost delta under basic curtailment further decreases by 6.4 EUR. In contrast, variable and smart curtailment experience a more modest reduction of 2.6 EUR and 2.5 EUR, respectively. Despite this, the cost savings remain above those realized by the TOU tariff.

All in all, the shift from the Fixed tariff to a time-variable tariff has a stronger economic impact than the choice of the curtailment strategy, even at higher EV penetration rates. This implies that introducing the RT tariff, even under basic curtailment, is more efficient than a Fixed tariff

or a TOU tariff. With an increasing EV penetration, however, a change from basic curtailment to smarter curtailment strategies becomes beneficial.

5. Discussion

This study uses a synthetically constructed distribution grid to represent a future scenario concerning household generation and consumption patterns. Due to the inherent heterogeneity of distribution grids in terms of size and topology, the applicability of the findings from this study to other contexts may be limited. However, certain trends and insights have emerged irrespective of the specific grid infrastructure.

The findings indicate that significant electric vehicle penetration does not necessarily cause grid congestion under the current market conditions, characterized by an absence of market and grid signals. For the analyzed use case, grid congestion occurs at EV penetration rates beyond 50% with a fixed tariff. This, however, is highly dependent on the respective grid topology and the current state of the expansion. IEA (2022a) find that, in German distribution grids, an EV penetration rate beyond 20% can cause significant grid adaption needs, affecting rural grids considerably stronger than urban grids. Transformers are by far the most affected grid element in this regard. An EV impact assessment study for Australia shows that depending on the grid, critical penetration rates vary significantly between 20% in rural and 80% in large urban distribution grids (Nacmanson et al., 2021). A similar study for California indicates that even EV penetration rates of 7% can cause significant overloading (Jenn and Highleyman, 2022). Rather than the EV penetration, the balance of regional demand and supply and the degree of correlation between EV load and the power generated by wind or PV systems determine how prone a distribution grid is to congestion. However, the probability of grid congestion rises due to the simultaneity of charging processes as the number of EVs increases (compare with Arnold et al. (2023))

Situations of abundant renewable feed-in are correlated with lower electricity prices. Flexible tariffs, which are driven by the electricity market prices, can thus help to integrate electricity from renewable resources, as they provide consumers with economic incentives to shift their demand to cheaper charging times with a high share of feed-in by renewables (compare with Powell et al.

(2022)). This is called market-oriented charging. The results of this passive coordination in the form of a price signal depend on the consumers' willingness to participate and pay.

Depending on the tariff design, purely market-oriented charging with a fully flexible electricity market retail price component could trigger herding behavior. It occurs when multiple users exploit the same low prices, resulting in higher loads in the respective time intervals. This would also be the case if a variable grid usage fee induces time-variability to the retail price and would be exacerbated by additional flexible consumers, such as heat pumps. ToU tariffs represent a trade-off between non-existing (Fixed tariff) and fully dynamic market signals (Real-Time tariff). They alleviate herding effects by incentivizing a shift of charging processes to certain time windows rather than specific points in time, as is the case with Real-Time tariffs. This finding is consistent with Schittekatte et al. (2022), who see in ToU tariffs a reasonable intermediate step toward fully flexible time-dependent tariffs.

We find that while variable tariffs cause significant load shifting, the consumers' resulting economic benefits are limited. For the chosen TOU tariff, households' cost savings are at about 1% compared to a flat tariff, while those for the RT tariff are at about 3%. This is due to the structure of retail prices, in which the electricity market component only has a small share, as electricity is taxed on a per-unit basis, and due to limited price fluctuations in the chosen use case. This is similar to Blaschke (2022), who makes the same observation for the current German electricity market. He finds that the average savings of flexible EV charging based on dynamic prices are about 22 EUR per year. In the presented future scenario, with a higher share of RES and resulting price volatility, the weighted average cost savings of EV charging with a fully dynamic tariff are 47.2 EUR per year. Herding effects highlight the limitations of variable market signals, as they can potentially exacerbate critical load situations. But, when market signals are paired with grid signals, grid constraints can be accounted for. However, curtailment dimensioning and planning become more complex due to the potential of passive control mechanisms to stimulate herding behavior. This complexity makes it challenging to curtail efficiently and system-oriented.

The proposed smart curtailment approach yields an optimal asset deployment considering both the electricity market and the grid. It intervenes only marginally with the purely market-oriented load

duration curve and maximizes the load while complying with grid limitations. It, thus, predominantly affects higher load levels nearing full load. It marks an optimal system-oriented benchmark that indicates the minimum flexibility requirements to fulfill the charging demand under consideration of the grid, regardless of the underlying tariff. It corresponds to volume signals with the highest possible degree of spatial and temporal differentiation on a node level. However, it remains a theoretical optimum, which is hard to implement due to the lack of transparency in distribution grids.

In distribution grids with low digitization and a lack of real-time load information, grid-oriented charging based on uniform volume signals to prevent congestion, e.g., ripple control signals is a common active control approach (basic curtailment). Fixed volume signals, with neither a spatial nor a temporal differentiation, are prone to inefficiencies since the curtailment rate might not be optimal, potentially leading to curtailment that exceeds peak load requirements. Furthermore, excessive curtailment could cause load loss if the grid signals are coordinated poorly with the market signals (Basic-RTT). Although we do not observe a loss of load in the presented use case, we do see that, dependent on the EV penetration rate, close to three times more load is shifted than ultimately necessary to comply with the grid limits under consideration of an RTT. With a more targeted curtailment approach (variable curtailment) with a high-level spatio-temporal differentiation on a subgrid level, we observe that the flexibility demand can be reduced considerably to an offset of about 37-38% above the minimum requirements.

At the same time, we observe that the interventions of DSO only marginally affect the potential cost savings of time-variable tariffs. For the TOU tariff, we see hardly any difference in the cost savings, as the defined intervals of the TOU tariff are long enough to shift the load in a grid-oriented fashion. We observe more nuanced differences between the curtailment strategies regarding cost savings for the RT tariff, which become more pronounced with increasing EV penetration. At a 70% EV penetration, the weighted average cost savings with basic curtailment compared to purely market-oriented charging reduce by 24%, while, with a reduction of about 10.5%, variable curtailment is considerably closer to smart curtailment (-8.5%). Given the limited potential of demand flexibility to achieve electricity cost savings but a considerable potential to avoid grid expansion (Spiliotis

et al., 2016; Resch et al., 2021), the real value of flexibility for households lies in avoiding grid expansion and, thus, higher grid usage fees.

Our results show that active control with volume signals can achieve feasible system states while complying with grid restrictions and avoiding loss of load, even if these are not necessarily optimal, depending on the curtailment strategy. However, without financial incentives, the acceptance of active control mechanisms is limited, as they restrict end use, impair consumer convenience, and potentially lead to, even if limited, a loss of profits, and as the necessary smart metering comes at a cost. A remuneration in case of curtailment, e.g., reduced grid usage fees, could overcome this. Nevertheless, effective coordination mechanisms between the market (electricity prices) and the grid (potential bottlenecks) cannot be overstated in ensuring the successful integration of EVs and other flexible assets. By integrating market incentives with grid constraints and capacity, we can foster user behaviors that uphold grid stability, contribute to integrating feed-in by renewable electricity resources, and provide economic benefits. It, thus, facilitates charging in a system-oriented manner. In the context of implementing curtailment strategies with spatiotemporal discrimination, it is imperative that, firstly, the state of the grid is measured, that, secondly, this information is disseminated to all relevant stakeholders, and that, thirdly, it is metered at the lowest possible cost. In this regard, digitizing distribution grids by implementing smart meters and digital control devices to deliver real-time data on load, grid capacity, and constraints is inevitable. To achieve this, questions about data sovereignty and access must be answered. Additionally, the costs of smart metering are an important factor in the business case of demand response. The calculated weighted average yearly cost savings of 47.2 EUR or lower, if the grid is considered, mark an upper acceptable bound for households with a flexible EV only.

Policymakers should foster an environment conducive to this transformation. First and foremost, policymakers need to speed up the digitization of German distribution grids and the smart meter roll-out, as smart meters are imperative for sophisticated charging concepts. Additionally, policymakers must work towards open regulation where grid and market information can be used jointly in future energy systems. This would involve rethinking the unbundling principle, which currently limits the potential for fully integrated systems.

6. Conclusion

As electrification of the transport sector progresses in the context of the global energy transition, fast and optimal integration of EVs into the existing energy system becomes crucial. While ensuring a market-oriented integration, the avoidance of grid congestion is imperative. For market-oriented EV charging, retailers use dynamic tariffs, incentivizing consumers to lower electricity costs by optimizing charging strategies based on those tariffs. However, due to herding behavior, this approach puts extra pressure on distribution grids, requiring DSOs to step in and curtail to prevent congestion. Design options for the intervention rights differ in the required information and the degree of spatio-temporal differentiation of the curtailment signals. The concrete design of DSO intervention rights is subject to political debate. We contribute to this by analyzing the implications of various active control approaches.

We have developed a model capable of assessing optimal charging strategies based on different tariff schemes, including fixed, Time-of-Use, and Real-Time tariffs. In the event of grid congestion concerns, we further explore various curtailment options by the DSO in optimizing charging strategies. The smart curtailment approach establishes an efficiency benchmark under the assumption of full information. Basic curtailment involves predefined curtailment factors in anticipation of congestion, while variable curtailment employs individual curtailment rates based on regional and temporal variations. By applying the model to a synthetic distribution grid configured with a future inventory of distributed assets, we show how different charging designs result in different grid loads, flexibility demands, and electricity costs.

Our research reveals that adopting time-variable tariffs yields marginal financial benefits for consumers. The weighted average cost savings amount to 47.2 EUR for the Real-time tariff and 16.9 EUR for the Time-of-Use tariff, representing only 1 to 3% of total electricity costs. However, we observe that time-variable tariffs, particularly at higher EV penetration rates, can induce herding behavior and increase peak load. To mitigate this issue, DSOs require intervention rights to prevent grid congestion effectively. Our findings indicate that all proposed intervention strategies

effectively prevent congestion, although notable differences exist in efficiency. The DSO's ability to convey differentiated signals, incorporating spatial and temporal nuances, closely correlates with the accuracy of the optimal benchmark. We show, that in the case of time-variable tariffs, the choice of the curtailment strategy is a stronger driver for flexibility requirements than the design of time-variable tariffs. From the end user's standpoint, curtailment has a negligible impact on charging costs, particularly with ToU tariffs. In the case of RT tariffs, cost savings diminish marginally after curtailment. Basic curtailment increases charging costs by 4.7 EUR per year, while variable curtailment only leads to a slightly lower increase by 2.6 EUR per year. The choice of the curtailment strategy becomes relevant at higher EV penetration rates, while time-variable tariffs benefit consumers regardless of the EV penetration rate.

Based on our research, we identify three relevant areas for further research. First, since this work focuses only on the flexibility of charging within a distribution grid, the interdependencies with other flexible consumers, such as heat pumps, should be analyzed. In this context, the efficiency of different coordination mechanisms can be analyzed as a contribution to the market design debate. Second, the value of flexibility use, abstracting from the selected use case, must be analyzed from a system perspective to obtain generalizable results. An analysis of the impact of flexible demand on market outcomes on spot markets is also of interest. Finally, the economic value of avoided grid expansion due to the use of flexibility should be the subject of further research to complement the discussion on the value of flexibility.

Acknowledgements

The authors would like to thank Marc Oliver Bettzüge, Johannes Wagner and Oliver Ruhnau for thoughtful and constructive comments and discussions on this work. This work also benefited from discussions at the research colloquium *Advanced Topics in Energy Economics and Informatics* at the University of Cologne, as well as the *29th Young Energy Economists and Engineers Seminar (YEEES)*.

Funding: This work was supported by the Ministry of Economic Affairs, Industry, Climate Protection and Energy of the State of North Rhine-Westphalia (MWIKE) within the project 'VISE - Smart: Data Generating added value through energy data - trends and transformation processes' (grant number EFO 0151D), as well as the German Federal Ministery of Economy and Climate protection within the project 'GreenVEgaS - Overall system analysis of sector coupling - economic evaluation of the energy infrastructure and generation for coupling the electricity, heat and transport sectors' (grant number 03EI1009C).

References

Arnold, F., Lilienkamp, A. and Namockel, N. (2023). Diffusion of electric vehicles and their flexibility potential for smoothing residual demand - A spatio-temporal analysis for Germany. *EWI Working Paper* 23/04.

Birk, S., Fleer, J., Holtz, G., Jeddi, S., Lilienkamp, A., Namockel, N., Schönfisch, M. and Wagner, D. J. (2021). Geschäftsmodelle für Regionale Virtuelle Kraftwerke. https://www.ewi.uni-koeln.de/cms/wp-content/uploads/2022/04/210420_VISE_Endbericht_v1.0.pdf.

Blaschke, M. J. (2022). Dynamic pricing of electricity: Enabling demand response in domestic households. *Energy Policy* 164: 112878, doi:https://doi.org/10.1016/j.enpol.2022.112878.

BNetzA (2023). Bundesnetzagentur. Festlegungsverfahren zur Integration von steuerbaren Verbrauchseinrichtungen und steuerbaren Netzanschlüssen nach § 14a Energiewirtschaftsgesetz. https://www.bundesnetzagentur.de/DE/Beschlusskammern/BK06/BK6_83_Zug_Mess/841_SteuVE/BK6_SteuVE_node.html.

Bonin, M. von, Dörre, E., Al-Khzouz, H., Braun, M. and Zhou, X. (2022). Impact of dynamic electricity tariff and home pv system incentives on electric vehicle charging behavior: Study on potential grid implications and economic effects for households. *Energies* 15, doi:10.3390/en15031079.

Daneshzand, F., Coker, P. J., Potter, B. and Smith, S. T. (2023). Ev smart charging: How tariff selection influences grid stress and carbon reduction. *Applied Energy* 348: 121482, doi:https://doi.org/10.1016/j.apenergy.2023.121482.

Dynge, M. F., Crespo del Granado, P., Hashemipour, N. and Korpås, M. (2021). Impact of local electricity markets and peer-to-peer trading on low-voltage grid operations. *Applied Energy* 301: 117404, doi:https://doi.org/10.1016/j.apenergy.2021.117404.

Englberger, S., Abo Gamra, K., Tepe, B., Schreiber, M., Jossen, A. and Hesse, H. (2021). Electric vehicle multi-use: Optimizing multiple value streams using mobile storage systems in a vehicle-to-grid context. *Applied Energy* 304: 117862, doi:https://doi.org/10.1016/j.apenergy.2021.117862.

European Comission (2010). Interpretative Note On Directive 2009/72/EC Concerning Common Rules For The Internal Market In Electricity And Directive 2009/73/EC Concerning Common Rules For The Internal Market In Natural Gas. Commission Staff Working Paper. https://energy.ec.europa.eu/system/files/2014-10/2010_01_21_the_unbundling_regime_0.pdf.

Frings, C. and Helgeson, B. (2022). Developing a Model for Consumer Management of Decentralized Options. *EWI Working Paper* 22/05.

Hecking, H., Kruse, J., Hennes, O., Wildgrube, T., Lencz, D., Hintermayer, M., Gierking, M., Peter, J. and Lorenczik, S. (2018). dena-Leitstudie Integrierte En-

ergiewende. https://www.dena.de/fileadmin/dena/Dokumente/Pdf/9261_dena-Leitstudie_Integrierte_Energiewende_lang.pdf.

Heilmann, C. and Wozabal, D. (2021). How much smart charging is smart? *Applied Energy* 291: 116813, doi:https://doi.org/10.1016/j.apenergy.2021.116813.

Helgeson, B. and Peter, J. (2020). The role of electricity in decarbonizing European road transport – Development and assessment of an integrated multi-sectoral model. *Applied Energy* 262, doi: https://doi.org/10.1016/j.apenergy.2019.114365.

IEA (2022a). Global EV Outlook 2022 - Securing supplies for an electric future. International Energy Agency, France. https://iea.blob.core.windows.net/assets/ad8fb04c-4f75-42fc-973a-6e54c8a4449a/GlobalElectricVehicleOutlook2022.pdf.

IEA (2022b). Grid Integration of Electric Vehicles - A manual for policy makers. International Energy Agency, France. https://iea.blob.core.windows.net/assets/21fe1dcb-c7ca-4e32-91d4-928715c9d14b/GridIntegrationofElectricVehicles.pdf.

IEA (2023a). Electricity Grids and Secure Energy Transitions, IEA, Paris , License: CC BY 4.0. https://www.iea.org/reports/electricity-grids-and-secure-energy-transitions.

IEA (2023b). Global EV Outlook 2023. International Energy Agency, France. https://iea.blob.core.windows.net/assets/dacf14d2-eabc-498a-8263-9f97fd5dc327/GEVO2023.pdf.

IEA (2023c). World Energy Outlook 2023. International Energy Agency, France. https://iea.blob.core.windows.net/assets/42b23c45-78bc-4482-b0f9-eb826ae2da3d/WorldEnergyOutlook2023.pdf.

Jenn, A. and Highleyman, J. (2022). Distribution grid impacts of electric vehicles: A california case study. *iScience* 25: 103686, doi:https://doi.org/10.1016/j.isci.2021.103686.

KBA (2023). Kraftfahrt-Bundesamt-Bestand. https://www.kba.de/DE/Statistik/Fahrzeuge/Bestand/bestand_node.html.

Kłos, M., Wawrzyniak, K. and Jakubek, M. (2015). Decomposition of power flow used for optimizing zonal configurations of energy market. In *2015 12th International Conference on the European Energy Market (EEM)*, 1–5, doi:10.1109/EEM.2015.7216779.

Meinecke, S., Sarajlić, D., Drauz, S. R., Klettke, A., Lauven, L.-P., Rehtanz, C., Moser, A. and Braun, M. (2020). SimBench — A Benchmark Dataset of Electric Power Systems to Compare Innovative Solutions Based on Power Flow Analysis. *Energies* 13, doi:10.3390/en13123290.

Nacmanson, D. W. J., Zhu, J. and Ochoa, P. L. (2021). Milestone 6: Network Modelling and EV Impact Assessment. Report UoM-ENA-C4NET-EV_Integration_M6_v03, Department of Electrical and Electronic Engineering at the University of Melbourne.

Pflugradt, N., Stenzel, P., Kotzur, L. and Stolten, D. (2022). Loadprofilegenerator: An agent-based behavior simulation for generating residential load profiles. *Journal of Open Source Software* 7: 3574, doi:10.21105/joss.03574.

Powell, S., Cezar, G. V., Min, L., Azevedo, I. M. L. and Rajagopal, R. (2022). Charging infrastructure access and operation to reduce the grid impacts of deep electric vehicle adoption. *Nature Energy* 7: 932–945, doi:10.1038/s41560-022-01105-7.

Resch, M., Bühler, J., Schachler, B. and Sumper, A. (2021). Techno-economic assessment of flexibility options versus grid expansion in distribution grids. *IEEE Transactions on Power Systems* 36: 3830–3839, doi:10.1109/TPWRS.2021.3055457.

Schittekatte, T., Mallapragada, D., Joskow, P. L. and Schmalensee, R. (2022). Electricity retail rate design in a decarbonizing economy: An analysis of time-of-use and critical peak pricing. *CEEPR Working Paper Series* 2022-015.

Schittekatte, T., Mallapragada, D., Joskow, P. L. and Schmalensee, R. (2023). Reforming retail electricity rates to facilitate economy-wide decarbonization. *Joule* .

Schnaars, D. P., Kienscherf, P. A., Gruber, K., Çam, D. E. and Schroer, K. (2022). EWI EV Preparedness Index. https://www.ewi.uni-koeln.de/en/publikationen/ev-preparedness/.

Schneider, M., Barrios, H. and Schnettler, A. (2018). Evaluation of unscheduled power flows in the European transmission system. In *2018 IEEE International Energy Conference (ENERGYCON)*, 1–6, doi:10.1109/ENERGYCON.2018.8398820.

Spiliotis, K., Ramos Gutierrez, A. I. and Belmans, R. (2016). Demand flexibility versus physical network expansions in distribution grids. *Applied Energy* 182: 613–624, doi:https://doi.org/10.1016/j.apenergy.2016.08.145.

Valogianni, K., Ketter, W., Collins, J. and Zhdanov, D. (2020). Sustainable electric vehicle charging using adaptive pricing. *Production and Operations Management* 29: 1550–1572, doi:https://doi.org/10.1111/poms.13179.

Nomenclature

Abbreviations

Table 3: Table of abbreviations

CHP	combined heat and power	EV	electric vehicle
DSO	distribution system operator	LV	low voltage
EASE	Electricity Asset Evaluation	MV	medium voltage
EM	electricity market	P2P	peer-to-peer
ESP	energy service provider	PV	photovoltaic

Sets, Parameters and Decision Variables

Table 4: Sets

Set	**Unit**	**Description**
$q \in Q$	-	Time
$c, c' \in G_{el}$	-	Component that generates electricity
$c, c' \in L_{el}$	-	Component that consumes electricity
$c, c' \in G_{th}$	-	Component that generates heat
$c, c' \in L_{th}$	-	Component that consumes heat
$n, m \in N$	-	Node
$n \in \alpha_c$	-	Set of nodes that belong to a component. Mapping nodes to components
$c \in \alpha_n$	-	Set of components that belong to a node. Mapping components to nodes
$k \in K$	-	Line

Table 5: Decision Variables

Variable	Unit	Description
$P_{c,q}^{g_{el}}$	kWh_{el}	Electrical energy generated by each generation unit c in time interval q
$P_{c,q}^{g_{el},s}$	kWh_{el}	Electrical energy generated by each generation unit c in time interval q and sold at the wholesale market
$P_{c,q}^{g_{el},f}$	kWh_{el}	Electrical energy generated by each generation unit c in time interval q and feed in to the grid
$P_{c,c',q}^{g_{el},p}$	kWh_{el}	Electrical energy generated by each generation unit c in time interval q and provided to a load c' on-site
$P_{c,q}^{l_{el}}$	kWh_{el}	Electrical energy consumed by each consumption unit c in time interval q
$P_{c,q}^{l_{el},p}$	kWh_{el}	Electrical energy procured from wholesale or an electricity provider and consumed by each consumption unit c in time interval q
$P_{c,c',q}^{l_{el}}$	kWh_{el}	Electrical energy procured from a generation unit c' on-site and consumed by each consumption unit c in time interval q
$P_{c,q}^{g_{th}}$	kWh_{th}	Thermal energy generated by each generation unit c in time interval q
$P_{c,c',q}^{g_{th}}$	kWh_{th}	Thermal energy generated by each generation unit c in time interval q and provided to consumption unit c'
$P_{c,q}^{l_{th}}$	kWh_{th}	Thermal energy consumed by each consumption unit c in time interval q
$P_{c,c',q}^{l_{th}}$	kWh_{th}	Thermal energy generated by generation unit c' and consumed by each consumption unit c in time interval q
$SOC_{c,q}^{el}$	kWh_{el}	Electrical energy inside a storage unit c in time interval q
$SOC_{c,q}^{th}$	kWh_{th}	Thermal energy inside a storage unit c in time interval q

Table 6: Parameters

Parameter	Unit	Description
A_d, A_u	-	Matrixes of flow distribution in the grid model
C_d, C_u	-	Matrixes of flow contribution in the grid model
$d_{c,q}$	-	grid connection of storage unit $[0; 1]$
e	-	factor that curtails maximum charging power
$F^{in}_{n,m}$	kW_{el}	Power injected in a bus m from a connected bus n in the grid model
$F^{out}_{n,m}$	kW_{el}	Power drained from bus n to a connected bus m in the grid model
$gdf_{k,n,q}$	-	Matrix with generation distribution factors
i^{el}_c	kW_{el}	installed capacity of each electrical component c
i^{th}_c	kW_{th}	installed capacity of each thermal component c
$i^{soc,el}_c$	kWh_{el}	installed capacity of each electrical storage c
$i^{soc,th}_c$	kWh_{th}	installed capacity of each thermal storage c
$ldf_{k,n,q}$	-	Matrix with load distribution factors
m^f_c	€$/kWh_{el}$	feed-in tariff for each generation unit c
m^l_c	€$/kWh_{el}$	subsidy for the own consumption of electricity generated by a chp unit c
$P^{act}_{k,q}$	kW_{el}	actual active power on a grid element
$P^{act,noControllable}_{k,q}$	kW_{el}	actual active power on a grid element affected by buses with non controllable assets
$P^{act,Controllable}_{k,q}$	kW_{el}	actual active power on a grid element affected by buses with controllable assets
$P^{gap,Controllable}_{k,q}$	kW_{el}	remaining active power on a grid element before capacity limit is reached
$P^{max,Controllable}_{k,q}$	kW_{el}	maximum active power of a grid element affected by buses with controllable assets
P_n	kW_{el}	Total nodal flow in the grid model
P^g_n	kW_{el}	Nodal generation in the grid model
P^l_n	kW_{el}	Nodal load in the grid model
p^w_q	€$/kWh_{el}$	wholesale price
$Q^{act}_{k,q}$	$kWAr_{el}$	actual reactive power on a grid element
$Q^{act,noControllable}_{k,q}$	$kWAr_{el}$	actual reactive power on a grid element affected by buses with non controllable assets
$Q^{act,Controllable}_{k,q}$	$kWAr_{el}$	actual reactive power on a grid element affected by buses with controllable assets
$Q^{gap,Controllable}_{k,q}$	$kWAr_{el}$	remaining reactive power on a grid element
$r_{c,q}$	kWh_{el}	Electrical energy that is consumed by electric vehicles through driving
s_q	-	time depended availability profile
$S^{max}_{k,q}$	VA	maximum apparent power of a grid element
t	€$/kWh_{el}$	taxes and levies
$\eta^{el}_{c,q}$	-	component-dependent and time-dependent electrical efficiency
$\eta^{th}_{c,q}$	-	component-dependent and time-dependent thermal efficiency
f_c	€$/kWh_{el}$	component-dependent fuel costs

Appendices

A. Calculation of maximum active power on each line and transformer

To formulate the equations (27) and (28) for the market model, the maximum active power for each line and transformer, only affected by nodes with controllable assets, has to be known. Based on the knowledge of the values for P^{act} and Q^{act} as a result of the AC power flow, the values of $P^{gap,Controllable}$ and $Q^{gap,Controllable}$ have to be calculated. It is assumed that the gap can only be controlled by readjusting the operation of assets which are part of the virtual power plant. Consequently, $Q^{gap,Controllable}$ is only affected by electric vehicles. As formulated in equation (17) the reactive power of loads is defined as a fixed ratio of active power. The variable $Q^{gap,Controllable}$ can therefore be replaced by the term $k * P^{gap,Controllable}$ where $P^{gap,Controllable}$ is the variable and k is the constant. The maximum apparent power can now be calculated as it is shown in equation (A.1).

$$S^{max} = \sqrt{(P^{act} + P^{gap,Controllable})^2 + (Q^{act} + Q^{gap,Controllable})^2} \tag{A.1}$$

To calculate the maximum value of $P^{gap,VPP}$ the equation (A.1) had to be transformed in order to apply the formula. The result is shown in equation (A.2). To simply this equation, the parameters a, b and c are introduced which represent the constant factors.

$$\begin{aligned} 0 = (1 + k^2) * P^{gap,Controllable^2} + (2P^{act} + 2kQ^{act}) * P^{gap,Controllable} + (P^{act^2} + Q^{act^2} + S^{max^2}) \\ = a * P^{gap,Controllable^2} + b * P^{gap,Controllable} + c \end{aligned} \tag{A.2}$$

Finally, the maximum additional active power $P^{max,Controllable}$ can be calculated by applying equation (A.3). The result $p^{gap,Controllable}$ can either be positive in case the line is not overloaded or negative, if the transmitted power has to be reduced.

$$P^{gap,Controllable} = \max[\frac{1}{2a} * (-b \pm \sqrt{b^2 - (4ac)})] \tag{A.3}$$

$$P^{max,Controllable} = (P^{act,Controllable} + P^{gap,Controllable}) * \eta \tag{A.4}$$

As a last step, the maximum active power that can be injected by nodes with controllable assets is calculated by adding $p^{max,Controllable}$ and $p^{gap,Controllable}$ as it is shown in equation (A.4). The factor η reflects a virtual buffer to additionally ensure that line loading does not exceed 100%. Its value is assumed to be equal 0.90.

B. Properties of the low voltage grids

						LV1	LV2	LV3	LV4	LV5	LV6
					Low voltage grid						
					Line length [m]	560	1467	1467	2352	2352	2352
					Number buses	14	96	96	128	128	128
					Transformer rated capacity [MVA]	0.16	0.25	0.25	0.40	0.40	0.40
					Maximum load without EVs [MW]	0.04	0.12	0.12	0.18	0.18	0.19
dRate 30					**Number EVs**	4	21	24	28	36	39
					EV penetration [%]	31	23	26	24	31	33
					Number of Households (HH)	13	93	93	118	118	118
	with	no BEV	no HP	no PV	no Storage	5	51	48	55	48	45
	with	BEV	no HP	no PV	no Storage	0	0	0	0	1	0
	with	no BEV	HP	no PV	no Storage	4	9	11	21	19	22
	with	BEV	no HP	PV	no Storage	0	0	0	0	0	0
	with	no BEV	HP	PV	no Storage	0	2	3	1	4	1
	with	no BEV	no HP	PV	Storage	0	5	6	11	10	7
	with	BEV	HP	no PV	Storage	1	9	12	11	15	23
	with	BEV	no HP	PV	Storage	0	0	0	0	0	0
	with	no BEV	HP	PV	Storage	0	5	2	2	1	4
	with	BEV	HP	PV	Storage	3	12	11	17	20	16
dRate 50					**Number EVs**	7	38	44	63	57	58
					EV penetration [%]	54	41	47	53	48	49
					Number of Households (HH)	13	93	93	118	118	118
	with	no BEV	no HP	no PV	no Storage	5	38	39	32	32	31
	with	BEV	no HP	no PV	no Storage	0	13	9	23	17	14
	with	no BEV	HP	no PV	no Storage	1	7	6	14	15	18
	with	BEV	no HP	PV	no Storage	3	2	5	7	4	4
	with	no BEV	HP	PV	no Storage	0	1	0	0	4	1
	with	no BEV	no HP	PV	Storage	0	4	4	8	9	7
	with	BEV	HP	no PV	Storage	1	10	15	12	15	23
	with	BEV	no HP	PV	Storage	0	1	2	3	1	0
	with	no BEV	HP	PV	Storage	0	5	1	1	1	3
	with	BEV	HP	PV	Storage	3	12	12	18	20	17
dRate 70					**Number EVs**	9	60	64	85	81	81
					EV penetration [%]	69	65	69	72	69	69
					Number of Households (HH)	13	93	93	118	118	118
	with	no BEV	no HP	no PV	no Storage	3	21	24	19	19	18
	with	BEV	no HP	no PV	no Storage	2	30	24	36	30	27
	with	no BEV	HP	no PV	no Storage	1	5	2	10	9	12
	with	BEV	no HP	PV	no Storage	3	4	9	11	10	10
	with	no BEV	HP	PV	no Storage	0	1	0	0	2	1
	with	no BEV	no HP	PV	Storage	0	2	3	4	7	3
	with	BEV	HP	no PV	Storage	1	10	15	12	17	23
	with	BEV	no HP	PV	Storage	0	3	3	7	3	4
	with	no BEV	HP	PV	Storage	0	4	1	0	0	3
	with	BEV	HP	PV	Storage	3	13	12	19	21	17

Figure B.1: Properties of low voltage grids 1-6 depending on the penetration rate of electric vehicles

						LV7	LV8	LV9	LV10	LV11	LV12
					Low voltage grid						
					Line length [m]	2352	746	746	746	1790	1078
					Number buses	128	43	43	43	110	58
					Transformer rated capacity [MVA]	0.40	0.40	0.40	0.40	0.63	0.63
					Maximum load without EVs [MW]	0.18	0.11	0.11	0.09	0.20	0.22
dRate 30					**Number EVs**	34	14	16	10	35	36
					EV penetration [%]	29	36	41	26	34	68
					Number of Households (HH)	118	39	39	39	104	53
	with	no BEV	no HP	no PV	no Storage	45	16	12	17	48	15
	with	BEV	no HP	no PV	no Storage	0	1	1	1	0	0
	with	no BEV	HP	no PV	no Storage	20	3	3	5	11	7
	with	BEV	no HP	PV	no Storage	0	0	0	0	0	0
	with	no BEV	HP	PV	no Storage	3	1	2	1	3	1
	with	no BEV	no HP	PV	Storage	14	3	5	3	6	3
	with	BEV	HP	no PV	Storage	21	8	7	5	18	7
	with	BEV	no HP	PV	Storage	0	0	0	0	0	0
	with	no BEV	HP	PV	Storage	2	2	1	3	1	2
	with	BEV	HP	PV	Storage	13	5	8	4	17	18
dRate 50					**Number EVs**	59	28	20	21	49	42
					EV penetration [%]	50	72	51	54	47	79
					Number of Households (HH)	118	39	39	39	104	53
	with	no BEV	no HP	no PV	no Storage	32	7	10	14	36	12
	with	BEV	no HP	no PV	no Storage	13	10	3	4	12	3
	with	no BEV	HP	no PV	no Storage	14	1	3	1	10	4
	with	BEV	no HP	PV	no Storage	6	2	0	4	1	3
	with	no BEV	HP	PV	no Storage	2	1	1	1	3	1
	with	no BEV	no HP	PV	Storage	10	1	4	1	6	3
	with	BEV	HP	no PV	Storage	22	8	8	5	18	7
	with	BEV	no HP	PV	Storage	4	2	1	2	0	0
	with	no BEV	HP	PV	Storage	1	1	1	1	0	2
	with	BEV	HP	PV	Storage	14	6	8	6	18	18
dRate 70					**Number EVs**	87	30	26	31	68	53
					EV penetration [%]	74	77	67	79	65	100
					Number of Households (HH)	118	39	39	39	104	53
	with	no BEV	no HP	no PV	no Storage	18	5	7	5	21	7
	with	BEV	no HP	no PV	no Storage	27	12	6	13	27	8
	with	no BEV	HP	no PV	no Storage	6	1	2	1	8	1
	with	BEV	no HP	PV	no Storage	14	2	1	4	3	6
	with	no BEV	HP	PV	no Storage	2	1	1	1	2	1
	with	no BEV	no HP	PV	Storage	5	1	3	0	5	2
	with	BEV	HP	no PV	Storage	22	8	8	5	19	7
	with	BEV	no HP	PV	Storage	9	2	2	3	1	1
	with	no BEV	HP	PV	Storage	0	1	0	1	0	0
	with	BEV	HP	PV	Storage	15	6	9	6	18	20

Figure B.2: Properties of low voltage grids 7-12 depending on the penetration rate of electric vehicles